

UNDERSTANDING THE MECHANISM OF ACTION OF RITUXIMAB™ IN THE
REVERSAL OF MULTIDRUG RESISTANCE IN A NON-HODGKINS LYMPHOMA
CELL LINE

APPROVED BY THE SUPERVISORY COMMITTEE

FEBRUARY 8, 2006

Ellen S. Vitetta
Ellen S. Vitetta, Ph.D.
Professor and Director, Cancer Immunobiology Ctr.

Maria-Ana Ghetie
Maria-Ana Ghetie, Ph.D.
Assistant Professor, Cancer Immunobiology Ctr.

Richard Anderson
Richard Anderson, Ph.D.
Professor and Chairman, Cell Biology

Nancy Monson
Nancy Monson, Ph.D.
Assistant Professor, Neurology

UNDERSTANDING THE MECHANISM OF ACTION OF RITUXIMAB™ IN THE
REVERSAL OF MULTIDRUG RESISTANCE IN A NON-HODGKINS LYMPHOMA
CELL LINE

by

Michelle C. Crank

DISSERTATION

Presented to the Faculty of the Medical School

The University of Texas Southwestern Medical Center at Dallas

In Partial Fulfillment of the Requirements

For the Degree of

DOCTOR OF MEDICINE WITH DISTINCTION IN RESEARCH

The University of Texas Southwestern Medical Center at Dallas

Dallas, Texas

February 8, 2006

ACKNOWLEDGEMENTS

I thank my mentors, Dr. Ellen Vitetta and Dr. Maria-Ana Ghetie, for their patience, knowledge, and willingness to teach. Their enthusiasm was contagious, and their sense of humor, a delightful surprise.

I thank Dr. Michael McPhaul and the UT Southwestern Medical Student Summer Research Program for the opportunity to work with such wonderful scientists while in medical school. I thank the Medical Student Research Forum for the opportunity to present my work to my peers and the faculty at UT Southwestern.

I thank my committee members, Dr. Richard Anderson and Dr. Nancy Monson, for their guidance and suggestions.

I thank Dr. Victor Ghetie for comments and discussions.

I thank my collaborator, Stephanie Kufert, for her work with all aspects of this project, and for teaching me so much about the mechanics of an immunology lab. I thank Joe Kufert for metabolic support. I thank Dr. Radu Marches for his work with the FRET experiments.

I thank Lien Le for purifying the monoclonal antibodies and Erica Garza and Linda Berry for administrative assistance.

I thank my parents for their encouragement, understanding and enthusiasm, from the very beginning. I thank my friends, especially Alison Beer, Janet Jacobson, and Shilpa Miniyar, for their help practicing presentations and willingness to listen to my running commentary on thesis number two. And I thank MS and HJV for their respective roles when this project began.

UNDERSTANDING THE MECHANISM OF ACTION OF RITUXIMAB™ IN THE
REVERSAL OF MULTIDRUG RESISTANCE IN A NON-HODGKINS LYMPHOMA
CELL LINE

Publication No. _____

Michelle C. Crank

The University of Texas Southwestern Medical Center at Dallas, 2006

Supervising Professors: Ellen S. Vitetta, Ph.D. and Maria-Ana Ghetie, Ph.D.

It has been previously demonstrated that an anti-CD20 monoclonal antibody (MAb) can reverse MDR in B lymphoma cells *in vitro*. However, the mechanisms underlying this effect are unknown. A recent study showed that anti-CD20 MAbs could induce rapid redistribution of CD20 into a detergent-insoluble membrane compartment (lipid rafts). By redistributing CD20 into rafts, Rituximab™ (RTX) modified their stability and organization. P-glycoprotein (P-gp) is the constituent protein of MDR tumor cells and is responsible for pumping chemotherapeutic agents out of cells. Because ~40% of P-gp is contained in lipid rafts, we hypothesized that when CD20 translocated into lipid rafts, it would displace P-gp. This displacement would lead to the reversal of MDR. To this end, we determined the function of the P-gp pump in the presence or absence of MAbs. In addition, the effects of dose and incubation time with MAbs and chemotherapeutic drugs were determined using Namalwa/MDR1 and three drug-sensitive cells. Finally, the

distribution of P-gp and CD20 in membranes was monitored after treatment with MAbs by western blot analysis.

We found that RTX inhibited the function of the P-gp pump while other anti-CD20 MAbs had no effect. RTX-mediated growth-inhibition of Namalwa/MDR1 cells was both dose- and time-dependent. Namalwa/MDR1 cells were resistant to doxorubicin and vincristine, but RTX rendered the Namalwa/MDR1 cells as chemosensitive as the parental Namalwa cells. RTX induced the translocation of CD20 into lipid rafts and the translocation of P-gp out of rafts. Our results supported our hypothesis that the ability of RTX to reverse MDR was initiated when CD20 was translocated into lipid rafts. This coincided with the translocation of P-gp out of rafts. When P-gp was no longer present in rafts, it lost activity and MDR was reversed.

LIST OF ABBREVIATIONS

ABC	ATP-binding cassette
ADCC	Antibody dependent cell cytotoxicity
APS	Ammonium persulfate
ATCC	American type culture collection
ATP	Adenosine triphosphate
BCA	Bicinchoninic acid
BCR	B cell antigen-specific receptor
BSA	Bovine serum albumin
CDC	Complement dependent cell cytotoxicity
CHOP	Cyclophosphamide, doxorubicin, vincristine, prednisone
cpm	Counts per minute
Cy	Cyanine
DRM	Detergent resistant membrane
ELISA	Enzyme-linked immunosorbent assay
FACS	Fluorescence activated cell sorting
FBS	Fetal bovine serum
FITC	Fluorescein isothiocyanate
FRET	Fluorescence resonance energy transfer
FU	Fluorouracil
GAMIg	Goat anti-mouse immunoglobulin
GPI	Glycosylphosphatidylinositol
h	Hours

HCl	Hydrochloric acid
HD	Hodgkin's disease
HRP	Horse radish peroxidase
Hz	Hertz
IC	Inhibitory concentration
IgG	Immunoglobulin G
IL	Interleukin
kDa	kiloDalton
MAb	Monoclonal antibody
M β CD	Methyl beta cyclodextrin
mcg	microgram
mCi	milliCurie
MDR	Multi-drug resistance
MES	4-methyl morpholine
MFI	Mean fluorescence intensity
mg	milligram
min	minutes
mL	milliliter
μ g	microgram
μ L	microliter
Na ₂ MoO ₄	Sodium molybdenum tetroxide
Na ₃ VO ₄	Sodium vanadate
NHL	Non-Hodgkins lymphoma

NK	Natural killer
nM	nanomolar
PBS	Phosphate buffered saline
PBSA	Phosphate buffered saline azide
P-gp	P-glycoprotein
PMSF	Phenylmethanesulphonylfluoride
RPM	Revolutions per minute
RPMI	Roswell park memorial institute
RTX	Rituximab TM
SCID	Severe combined immunodeficiency
SDS	Sodium dodecyl sulfate
SOCC	Store-operated calcium channel
TEMED	Tetramethylethylenediamine
WB	Western blot
WHO	World Health Organization
x g	times gravity

TABLE OF CONTENTS

ACKNOWLEDGEMENTS	III
ABSTRACT	IV
LIST OF ABBREVIATIONS	VI
TABLE OF CONTENTS	IX
LIST OF FIGURES	XII
LIST OF TABLES	XIII
INTRODUCTION	1
NON-HODGKIN’S LYMPHOMA	1
MONOCLONAL ANTIBODIES IN CANCER THERAPY	2
MULTIPLE DRUG RESISTANCE (MDR)	3
RTX	5
CD20	6
LIPID RAFTS	7
HD37 CHEMOSENSITIZES MDR CELLS	10
AIMS OF THIS STUDY	11
MATERIALS AND METHODS	13
CELL LINES	13
ANTIBODIES AND REAGENTS	13
CHEMOTHERAPEUTIC DRUGS	14
FLOW CYTOMETRY	14
GROWTH INHIBITION	15

CELLULAR INFLUX AND EFFLUX ASSAYS	16
CYTOTOXICITY ASSAY	17
PREPARATION AND ANALYSIS OF LIPID RAFTS FOR WESTERN BLOT.	19
BCA PROTEIN ASSAY	21
WB ANALYSIS	21
RESULTS	24
RTX MODESTLY INHIBITED THE GROWTH OF BOTH P-GP ⁺ AND P-GP ⁻ CELLS	25
RTX CHEMOSENSITIZED NAMALWA/MDR1 CELLS	26
RTX INHIBITED THE CELLULAR EFFLUX OF RHODAMINE-123 AS EFFECTIVELY AS VERAPAMIL	29
RTX INDUCED THE TRANSLOCATION OF P-GP OUT OF LIPID RAFTS	31
RTX INDUCED THE TRANSLOCATION OF CD20 INTO LIPID RAFTS	35
DISCUSSION	37
GENERAL	37
OBJECTIVES AND MAJOR FINDINGS	37
RTX MODESTLY INHIBITED THE GROWTH OF P-GP ⁺ AND P-GP ⁻ B-NHL CELLS <i>IN VITRO</i>	38
RTX CHEMOSENSITIZED NAMALWA/MDR1 CELLS	40
RTX INHIBITED THE ACTIVITY OF THE P-GP PUMP	41
RTX INDUCED THE TRANSLOCATION OF P-GP OUT OF LIPID RAFTS AND THE TRANSLOCATION OF CD20 INTO LIPID RAFTS	43
FUTURE DIRECTIONS	50
CONCLUSIONS	50

REFERENCES	52
VITAE	63
PUBLICATIONS	65

LIST OF FIGURES

FIGURE 1. MECHANISMS UNDERLYING MDR..	4
FIGURE 2. THE COMPOSITION OF LIPID RAFTS.....	9
FIGURE 3. THE GROWTH OF P-GP ⁺ AND P-GP ⁻ CELLS CULTURED WITH AND WITHOUT RTX..	26
FIGURE 4. THE CYTOTOXIC EFFECT OF RTX ON P-GP ⁺ AND P-GP ⁻ NAMALWA CELLS..	27
FIGURE 5. THE RHODAMINE-123 DYE EFFLUX ASSAY TO MEASURE P-GP ACTIVITY.	29
FIGURE 6. THE EFFECT OF RTX ON P-GP-MEDIATED RHODAMINE-123 EFFLUX BY MDR1 CELLS.....	30
FIGURE 7. PREPARATION OF LIPID RAFTS FOR WB ANALYSIS..	33
FIGURE 8. WB ANALYSIS OF THE DISTRIBUTION OF P-GP IN LIPID RAFTS IN NAMALWA / MDR1 CELLS BEFORE AND AFTER INCUBATION WITH MABS.....	34
FIGURE 9. WB ANALYSIS OF THE DISTRIBUTION OF CD20 IN LIPID RAFTS IN NAMALWA/MDR1 CELLS BEFORE AND AFTER INCUBATION WITH MABS	35
FIGURE 10. MODEL OF THE EFFECT OF RTX BINDING TO CD20 ON P-GP AND LIPID RAFTS.	48

LIST OF TABLES

TABLE 1. THE EXPRESSION OF CD20 AND P-GP ON THE SURFACE OF NAMALWA/MDR1 AND PARENTAL (MDR1 ⁻) NAMALWA CELLS.....	24
---	----

INTRODUCTION

Non-Hodgkin's Lymphoma

Malignancies of hematopoietic cells have been divided into leukemias, which are malignancies of the blood and bone marrow, and lymphomas, which are predominately “solid” tumors of the lymph nodes. Lymphomas were originally subdivided into Hodgkin's disease (HD) and Non-Hodgkin's lymphoma (NHL) based upon the presence of Reed-Sternberg cells in HD and their absence in NHL. The further classification of NHL has been debated throughout the past century. The most recent classification scheme, created by the WHO in 1999, utilized morphologic, clinical, immunologic, and genetic information to divide NHL and other lymphoid malignancies into malignancies with clinical and therapeutic relevance. [1, 2] Clinically, lymphomas have been characterized as indolent or aggressive, based upon their rate of progression. NHL has been subdivided into B and T cell lymphomas, and within each of these lineages what stage of normal development the cancer cells most resemble, based upon the immunologic characteristics of the malignant cells. Specific cytogenetic translocations have been used to differentiate subtypes of NHL, for example, (t 8:14) is found in Burkitt's lymphoma, and (t 14:18) is common in follicular lymphoma.

For unknown reasons, NHL increased in frequency in the United States at the rate of 4% per year between 1950 and the late 1990s. However, the rate of increase in the past few years has plateaued. About 54,000 new cases of NHL were diagnosed in the United States in the year 2004. NHL was more frequent in the elderly and in men. Patients with both primary and secondary immunodeficiency states were predisposed to developing NHL. These included patients with HIV infection, inherited immune deficiencies,

rheumatoid arthritis, and patients who have undergone organ transplantation. The incidence of NHL and the patterns of expression of the various subtypes differed geographically. T cell lymphomas were more common in Asia than in western countries, while certain subtypes of B cell lymphomas, such as follicular lymphoma, were more common in western countries.[3]

Monoclonal Antibodies in Cancer Therapy

Monoclonal antibodies (MAbs) have become an essential tool in the treatment of many cancers. Their specificity and low toxicity have contributed to improved quality of life and prolonged survival for patients. MAbs can operate by inducing cell cycle arrest or apoptosis, inhibiting angiogenesis, blocking the binding of tumor cells to the extracellular matrix, and recruiting effector cells and molecules.[4] MAbs are unique because they can often exert their therapeutic effect by more than one of these mechanisms.[5] In addition, MAbs can be modified to enhance their therapeutic effect by increasing their affinity or avidity, improving their binding to certain Fc receptors, improving tumor penetration, altering the half-life of the MAb, and/or conjugating them to a toxic payload such as a drug, prodrug, toxin or a radionuclide.[4, 6, 7]

The success of MAbs was evident from the approval by the FDA (since 1997) of five unconjugated and two conjugated MAbs, for cancer therapy. Over 135 MAbs are now being evaluated in clinical trials. RituximabTM/RituxanTM (RTX), a chimerized anti-CD20 antibody, was the first MAb approved by the FDA for the treatment of cancer, specifically non-Hodgkin's lymphoma.[8] Campath, a humanized anti-CD52 antibody, was approved for the treatment of chronic lymphocytic leukemia.[9] Herceptin, a humanized anti-HER-2/neu antibody, was approved for the treatment of metastatic breast

cancer.[6, 7, 10] Avastin, a humanized anti-VEGF antibody, and Erbitux, a chimeric anti-EGFR antibody, were approved for the treatment of colorectal cancer.[11, 12] Two MAbs conjugated to radioisotopes were also recently approved. Bexxar,TM conjugated to ¹³¹I, and Zevalin,TM conjugated to ⁹⁰Y, are anti-CD20 MAbs now being used to treat NHL.[13, 14] The potential of MAbs has not been fully explored even in the cancers for which they have been approved. Studies are ongoing to elucidate their mechanisms of action, in order to optimize their use.[15-17] Applications of MAbs to other malignancies as well as autoimmunity, infectious diseases, and graft vs. host diseases are under investigation.[18-20]

Multiple Drug Resistance (MDR)

MDR has been identified in many types of cancer, both at diagnosis and after treatment with chemotherapeutic agents.[21] The development of MDR in lymphoma cells correlates with the decreased success of chemotherapy, both in newly diagnosed patients and in patients who have failed previous therapy.[22, 23] There are multiple mechanisms that contribute to MDR, including two that have been well characterized. **(Figure 1)** These include decreased permeability of the cell membrane to chemotherapeutic agents and over-expression of the membrane protein, P-glycoprotein (P-gp.)[24] P-gp is encoded by the human *MDR1* gene and is one of several proteins contributing to the MDR phenotype that belong to the ATP-binding cassette (ABC) superfamily, which hydrolyze ATP.[24, 25] These proteins act as pumps that decrease the intracellular accumulation of chemotherapeutic drugs. P-gp is also expressed on some

normal tissues, including brain, intestine, adrenal cortex, placenta, hematopoietic stem cells, liver and kidney.[26]

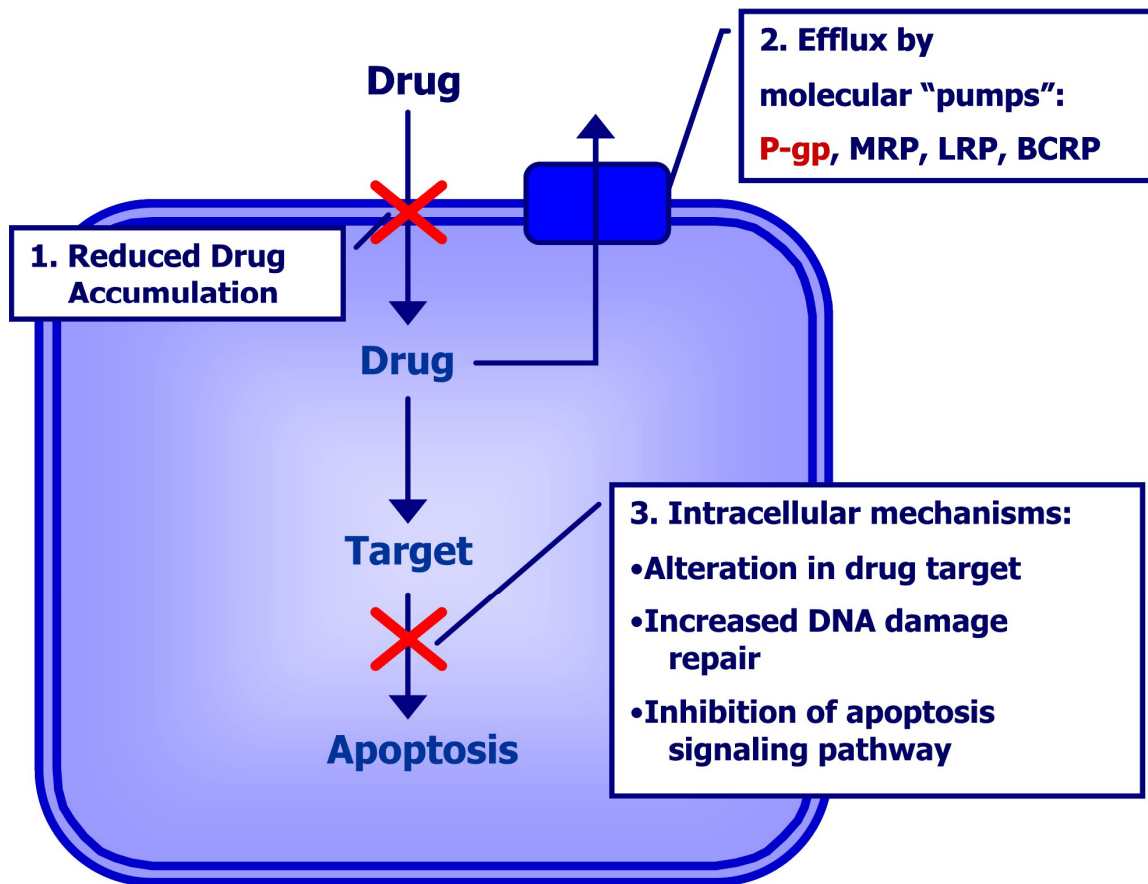


Figure 1. Mechanisms Underlying MDR. MDR develops after treatment with chemotherapy, and it can occur by several mechanisms. These include reduced drug accumulation, efflux of drug by molecular “pumps” in the membrane, intracellular alterations in drug targets, increases in the ability of cells to repair DNA damage, and inhibition of the signaling pathways leading to apoptosis.

Attempts to overcome MDR have been made since the phenomenon was recognized in the 1970's. Several inhibitors of P-gp activity have been characterized, including Cyclosporine A, Verapamil, progesterone, and Solutol HS-15. [24] These modifiers all have the problem of side effects, because they alter the activity of P-gp in normal tissues as well as MDR cancer cells. [27] Several alter the pharmacokinetics of

chemotherapeutic agents, necessitating reductions in dosage of these agents to compensate for slower drug clearance from the body. Targeted modifiers of P-gp activity, such as MAbs directed against cancer cells, would decrease problems with side effects and altered drug pharmacokinetics that currently limit the use of the non-targeted modifiers. In addition, MAbs themselves have low toxicity, and their use would reduce the dosage of chemotherapeutic agents required to kill cancer cells, thus reducing their toxicity in patients.

RTX

Because RTX was the first MAb to be approved by the FDA for the treatment of cancer, RTX has been extensively studied both *in vitro* and *in vivo*. [28] It is a chimeric, IgG1 anti-CD20 MAb that combines murine heavy and light chain variable regions with human heavy and light chain constant regions. [29] RTX was approved in the U.S. for the treatment of relapsed or refractory, low-grade or follicular, B-cell NHL. [29] In Europe, it was approved for use in relapsed stage III/IV follicular NHL. [30] In the pivotal trial for FDA approval of RTX, the overall response rate was 50% when RTX was used as a single agent, [30, 31] and the overall response rate was >95% when RTX was used in combination with chemotherapy. [32] A decade later, patients treated with RTX combined with chemotherapy for low grade or follicular lymphoma and large cell lymphoma showed prolonged time to progression of disease and longer periods of disease-free survival. [33, 34] These results were promising for the long-term survival of patients with NHL who traditionally had a poor long-term prognosis. [35]

In vitro studies, as well as studies in both animals and humans, suggested that the antitumor activity of RTX was mediated by antibody-dependent cellular cytotoxicity (ADCC) or complement-dependent cytotoxicity (CDC). [29, 30, 36] RTX also had direct anti-proliferative effects on cancer cells, and, in some instances, it induced apoptosis [36, 37] in lymphoma cell lines with bcl2 gene rearrangements. [38, 39] RTX was also shown to chemosensitize drug-resistant cells. Investigations into the mechanism(s) underlying the anti-tumor activity of RTX as a single agent and in combination with chemotherapy are ongoing. By understanding these mechanisms, it might be possible to further enhance current cell killing strategies or develop novel agents and strategies. Recent clinical trials included combining IL-2 or GCSF with RTX to enhance ADCC, [40, 41] and treating relapsed patients with RTX before or after autologous stem cell transplant to eliminate contaminating lymphoma cells. [42]

CD20

CD20 is a membrane-embedded phosphoprotein expressed on the surface of B cells. [43] It is expressed at high levels by pre-B through mature B cells, but not by hematopoietic stem cells or antibody-producing plasma cells. Activated B cells have higher expression than naive B cells. [43] When CD20 is bound to anti-CD20 antibodies, it internalizes poorly. It is not present in the circulation. The 33-37 kDa CD20 glycoprotein contains four hydrophobic, membrane-spanning regions as well as a small extracellular domain and cytoplasmic N- and C-terminal ends. [44] It forms dimers and tetramers after chemical cross-linking, and it has been found to assemble into a 200-kDa complex in the cell membrane. [45, 46] It functions as a store-operated calcium channel (SOCC)

activated by the B cell receptor (BCR), which contributes to sustained elevation of cytoplasmic free calcium required for B cell activation. [47]

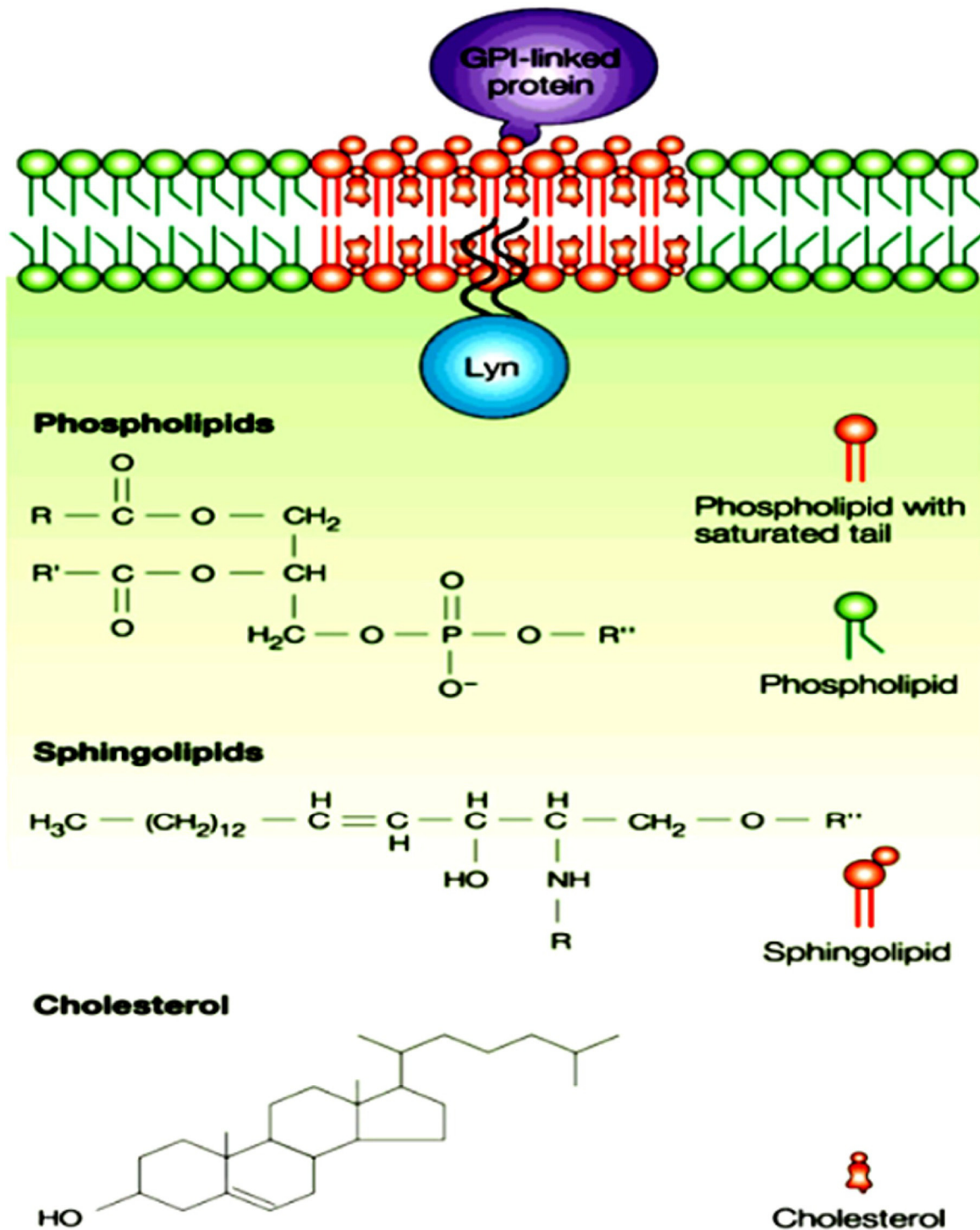
In addition to Rituximab™, several other anti-CD20 MAbs have been investigated. They recognize distinct epitopes on the CD20 molecule, and they have varying effects on the cell. Some trigger resting B cells to enter the cell cycle or induce IgM production, while others prevent cell cycle progression and activation or differentiation, and others cause cell death. [43] RTX and other anti-neoplastic MAbs belong to the latter group. These MAbs have been classified according to their effect on the location of CD20 in the plasma membrane, as well as on B cell proliferation and differentiation. One group, including RTX and 1F5, induce the translocation of CD20 into lipid rafts, a detergent-insoluble portion of the cell membrane. Another group of MAbs including B1, the MAb used in Bexxar,™ does not appear to induce this translocation of CD20 within the membrane. [48] The mechanism of interaction of these MAbs with CD20 is still under investigation, in the hopes that a more complete understanding of how the MAbs act will enable development of better treatment strategies for a wide range of diseases and the design of better MAbs.

Lipid Rafts

The cell membrane is made up of lipids with different physical and chemical properties that can aggregate to form heterogeneous areas, or domains, some of which have been termed lipid rafts. [49] Lipid rafts have been originally defined as detergent resistant membrane (DRM) fractions, which are insoluble in Triton X-100. [50] After extraction, the lower-density rafts can be separated from other cell membrane components by

ultracentrifugation along a density gradient. Raft domains contain a high proportion of cholesterol and saturated phospho- and sphingolipids, which allow for tighter packing and a more ordered structure than that found elsewhere in the cell membrane. [51]

(Figure 2) Certain proteins also preferentially aggregate in lipid rafts, including glycosylphosphatidylinositol (GPI)-anchored proteins, Src-family tyrosine kinases, flotillins, caveolins, heterotrimeric G proteins, and annexins. [52-56] Many functions have been proposed for rafts, including cellular adhesion, endocytosis, the budding of viral particles, and cell signaling. [49]



R, R', Hydrocarbon chains of fatty acids
 R'', Head group
 GPI, glycosylphosphatidyl inositol

Figure 2. The composition of Lipid Rafts. The membrane can be operationally divided into domains called lipid rafts (red), which contain a high proportion of cholesterol, saturated phospholipids, and

sphingolipids. Lipid rafts are platforms for signaling. The remainder of the membrane, (green), is soluble in certain detergents, while rafts are not. Rafts and the soluble fraction can be physically separated by lysing cells and carrying out density gradient-centrifugation on the cell lysates. (From Pierce, Susan K. Lipid Rafts and B-Cell Activation. **Nature Reviews Immunology**, Vol. 2, Feb 2002. Pp. 96-105). CD20 has been localized in lipid rafts under certain experimental conditions. [57-59]

When Triton X-100 is used to isolate lipid rafts from the remainder of the cell membrane, CD20 is not localized to the lipid rafts. But when cells are incubated with certain MAbs (including RTX) prior to treatment with Triton X, CD20 is then found in lipid rafts. It has been noted by some investigators that when different detergents are used, CD20 is constitutively present in lipid rafts, even in the absence of MAb treatment. [47, 60] Hence the lipid rafts are operationally defined by their solubility in different detergents, although Triton X is the detergent most frequently used. The mechanism(s) underlying the translocation of CD20 have yet to be elucidated. P-gp is also present in lipid rafts. [61, 62] Its function as a pump is affected by its lipid environment, though there is some conflicting information on the effects induced by various changes in the membrane, such as cholesterol extraction. [63-66] Investigation into the relationship of both CD20 and P-gp in lipid rafts and their interactions with their lipid environment is ongoing.

HD37 chemosensitizes MDR cells

Previous work in our laboratory investigated the effect of the anti-CD19 MAb, HD37, on the activity of P-gp in MDR NHL cells.[67] CD19 is another protein found on the surface of most B cells, which is a target for multiple MAbs. HD37 inhibited the activity of P-gp in Namalwa/MDR1 cells with ~50% of the efficiency of verapamil, a well-known inhibitor of P-gp activity. The inhibitory activity of HD37 did not require an Fc portion.

F(ab')₂ fragments were effective, but Fab' fragments were not, suggesting that higher avidity binding and/or cross-linking of CD19 were necessary for the effect. We could find no evidence that HD37 recognized a cross-reactive epitope on P-gp, modulated P-gp from the cell surface, or enhanced the ATPase activity of membranes from treated cells. Further investigation suggested mechanisms responsible for the effect of HD37 on the P-gp pump. [68] Using fluorescence resonance energy transfer (FRET), CD19 and P-gp were demonstrated to be constitutively associated in cells. In the absence of treatment with anti-CD19, 40% of P-gp molecules expressed by Namalwa/MDR1 cells resided in lipid rafts. Following treatment of the cells with HD37 and disruption of the interactions between P-gp and CD19, P-gp translocated out of lipid rafts and CD19 translocated into lipid rafts. These results suggested that anti-CD19 might chemosensitize P-gp⁺ cells by interfering with interactions between CD19 and P-gp, rapidly resulting in the translocation of P-gp into a compartment on the plasma membrane where it is no longer active.

Aims of this study

The objectives of this study were as follows: 1) to confirm that Namalwa/MDR1 cells expressed P-gp and CD20 and whether expression changed after time in culture, 2) to determine the effect of RTX on the growth of Namalwa/MDR1 and parental Namalwa cells, 3) to determine the effect of RTX on the killing of Namalwa/MDR1 cells with and without chemotherapeutic drugs, 4) to determine the effect of RTX on the activity of the P-gp pump, 5) to determine whether RTX altered the membrane distribution of P-gp such that it could no longer function as an active pump. To this end, we studied the distribution

of P-gp and CD20 in lipid rafts vs. the soluble fraction of the cell membrane before and after treatment of MDR1 cells with RTX.

MATERIALS AND METHODS

Cell lines

The human Burkitt's lymphoma cell line, Namalwa, was infected with a human *MDR1* gene-containing retrovirus (Namalwa/MDR1), and was a gift from Dr. R. O'Connor at ImmunoGen (Boston, MA). The human Burkitt's lymphoma cell line, Ramos (American Type Culture Collection (ATCC)[®] Number: CRL-1596[™], Manassas, VA), was purchased. [69] Both the parental P-gp- Namalwa cells and the P-gp+ Namalwa/MDR1 cells were maintained in culture in complete RPMI-1640 medium (Sigma-Aldrich, St. Louis, MO) containing 7.5% heat-inactivated fetal bovine serum (FBS) (HyClone, Logan, UT) supplemented with 20 mM HEPES (Sigma, St. Louis, MO), 100 units/ml penicillin (GIBCO/Invitrogen, Carlsbad, CA), 100 µg/ml streptomycin (GIBCO), and 100 mM L-glutamine (GIBCO) (complete medium). Cells were grown in a humidified atmosphere of 5% CO₂ and air, and viability was determined by trypan blue exclusion. Cells were diluted 1:1 with trypan blue (0.04% in sterile phosphate-buffered saline (PBS)) and counted using a hemacytometer (Bright-Line, Reichert-Jung, Horshan, PA). Viability was calculated by the equation $100 \times (\# \text{ viable cells}) / (\# \text{ viable cells} + \# \text{ non-viable cells})$. Cell lines were maintained in culture for 6 weeks and were then replaced with frozen stock. The cellular phenotype was determined by flow cytometry.

Antibodies and Reagents

The following MAbs or hybridomas were used: (a) anti-CD20 (RTX) was purchased from Genentech (San Francisco, CA); (b) anti-P-gp (UIC2) from Immunotech, Miami, FL. recognized an epitope on P-gp which interferes with its function; (c) anti-CD22 (RFB4)

from Dr. G. Janossy, Royal Free Hospital, London, UK was used as control antibody, which binds to CD22 on Namalwa/MDR1 cells but does not chemosensitize them; UV22-2, a hybridoma generated in our lab was prepared, purified and used as a control antibody. (d) Fluorescein Isothiocyanate (FITC)-goat anti-mouse IgG (H+L) (GAMIg) was purchased from Kirkegaard & Perry Laboratory, Inc., Gaithersburg, MD. For Western Blots (WB) we used the antibodies indicated below and the detection kit provided by ECI Western Blotting Analysis System, Amersham Pharmacia, UK.

Chemotherapeutic drugs

Doxorubicin (hydrochloride injection, USP) was purchased from Gensia Sicor Pharmaceuticals, Inc. (Irvine, CA) and Vincristine sulfate (injection, USP) was purchased from Faulding Pharmaceutical Co. (a Mayne Group Company, Paramus, NJ).

Flow cytometry

Indirect immunofluorescence assays were carried out to evaluate the binding of anti-P-gp and anti-CD20 MAbs to both the Namalwa and the Namalwa/MDR1 cell lines. Indirect immunofluorescence assays were carried out using RTX, UIC2, UV22-2, and RFB4, and FITC-GAMIg. Cells (10^6 per sample) were collected in a 50 ml conical tube (BD Falcon, San Jose, CA) centrifuged (Sorvall RC3C Centrifuge) for 6 min at 419 x g, washed in phosphate-buffered saline + 0.01% sodium azide (PBSA) at 4 °C, centrifuged again (6 min at 419 x g at 4 °C) and resuspended in PBSA at 10^7 cells/ml. All materials were kept on ice from this point on. 100 μ L of the cell suspension was placed in each tube (12 X 75, round bottom, BD Falcon, San Jose, CA). MAbs (1–10 mg) were added to each tube,

tubes were vortexed, and then they were incubated in the dark for 15 min on ice, vortexed, then incubated for 15 more min under the same conditions. Then, 800 μ L PBSA was added to each tube, and tubes were centrifuged (6 min at 419 x g). After supernatants were aspirated, the cells were washed again with complete medium containing 0.01% sodium azide, resuspended in 100 ml of medium, and 2–3 ml of FITC-GAMIg was added to each tube. Tubes were vortexed and then incubated on ice for 30 min. The cells were washed twice in 800 μ L medium with 0.01% sodium azide, resuspended in 500 μ L of the same medium, and analyzed on the FACS (FACScan; Becton Dickinson, Mountain View, CA).

Growth Inhibition

Namalwa/MDR1 and Ramos cells were grown in the presence of RTX to study the effect of the antibodies on cell growth. Cells were collected in a 50 mL conical tube (BD Falcon, San Jose, CA) and centrifuged at 300 x g for 10 min at 4°C (Sorvall Centrifuge, RC3C, DuPont, Wilmington, DE). The cells were resuspended in complete medium without fetal bovine serum (FBS), at 2×10^5 cells/mL and centrifuged again under the same conditions to wash the cells. Then the cells were resuspended in complete medium with 10% FBS at 5×10^5 cells/mL and 5 mL of cells were seeded into a 25 cm² tissue culture flask (BD Falcon, San Jose, CA), using one flask for each treatment condition. One flask of untreated cells served as the control. Treatment conditions included concentrations of RTX varying from 1 - 500 μ g/mL or 7×10^{-9} – 3.4×10^{-6} M. The MAb was added from stock solution (12.2 mg/mL RTX) or for lower concentration, stock was diluted first in a sterile PBS solution. All dilutions were made at high concentration (≥ 1

mg/mL) so as not to dilute cell medium when MAbs were added. Cells were incubated at 37°C in 5% CO₂/95% air for 5-10 days. Cells were counted daily and viability was determined using Trypan blue exclusion. Cells were replenished daily with RTX to maintain a steady concentration of antibody. Cells were discarded when viability dropped to <50%. Experiments were repeated 5 times.

Cellular Influx and Efflux Assays

To study the function of the P-gp pump on Namalwa/MDR1 cells, Rhodamine 123 was used in an efflux assay. Namalwa/MDR1 cells (1×10^6 /treatment) were collected, pelleted (as described in “Flow Cytometry,”) washed once in serum-free medium, and resuspended in 1.8 ml of serum-free medium in a clear tube (12 X 75, round bottom, BD Falcon, San Jose, CA). RTX was diluted from stock (12.2 mg/mL) in medium to 0.15 mg/mL. 200 µL of RTX was then added to the cells. Two additional samples of cells were incubated in medium alone during this time as negative controls. To a final sample, 200 µL of Verapamil (100 µM in RPMI 1640, Sigma, St. Louis, MO) was added as a positive control. All samples were incubated with rotation (50 Hz, LabQuake Shaker, Berkeley, CA) for 1 h at 37°C. Cells were then pelleted and washed twice with 2 mL of serum-free medium. They were resuspended in 0.9 mL of serum-free medium.

1. Influx: To the sample previously treated with RTX, 100 µL of RTX (0.15 mg/mL) was added along with 5 µL Rhodamine 123 (100 µg/mL in sterile saline, Sigma, St. Louis, MO). To one negative control, 100 µL of serum-free medium was added. To the second negative control, 100 µL of medium plus 5 µL of Rhodamine 123 was added. To the positive control, 100 µL of Verapamil (100 µM in RPMI 1640) plus 5 µL of

Rhodamine 123 was added. All samples were incubated for 1 hour at 37°C with rotation (50 Hz, LabQuake Shaker, Berkeley, CA). The cells were pelleted and washed twice with 2 mL/sample of serum-free medium, then resuspended in 0.9 mL of serum-free medium.

2. Efflux: Rhodamine 123 loaded cells were re-cultured at 37°C for 2 h. Cells were pelleted, washed twice in 2 mL PBSA, and resuspended in 1.5 mL PBSA. Samples were analyzed on the FACScan by accumulating events in the FL1 channel. The efflux rate of Rhodamine 123 was determined. After 2 h, efflux was complete. We, therefore, chose 2 h as the standard conditions for the assay. To quantitate the effect of treatment with RTX on Rhodamine 123 efflux from Namalwa/MDR1 cells, we measured the shift of the histogram to the right as compared with the negative control (Rhodamine 123 only). The effect of Verapamil (positive control) was taken as 100%, and the effect of RTX was calculated as a percentage of the change induced by Verapamil. The experiment was repeated 5 times.

Cytotoxicity assay

The cytotoxicities of doxorubicin and Vincristine were tested on both Namalwa and Namalwa/MDR1 cells. The effect of MAbs (RTX and RFB4) on doxorubicin- or Vincristine-mediated cytotoxicity was also evaluated using a [³H]-Thymidine incorporation assay.

Both Namalwa and Namalwa/MDR1 cells were centrifuged for 10 min at 300 x g at 4°C (Sorvall RC3C centrifuge). The cells were washed with complete medium without FBS and centrifuged again as above. The cells were resuspended in complete medium without FBS at 1.4×10^5 cells/mL (Namalwa/MDR1) and 1.7×10^5 cells/mL (Namalwa). RTX

(12.2 mg/mL stock) was added to cells to bring concentrations to 0.2 mg/mL.

Concentrated cells (without MAb) were used as the positive controls. Doxorubicin was diluted in complete medium without FBS via serial dilutions to final concentrations of 10-120 nM. 100 μ L of each serial dilution of doxorubicin was added to each well of a 96-well tissue culture plate (BD Falcon, San Jose, CA). 100 μ L of complete medium was used as a negative control. Then 100 μ L of the appropriate cell suspension was added to each well, giving final concentrations of doxorubicin of 5-60 nM and a final concentration of RTX of 0.1 mg/mL or 7×10^{-7} M. Plates were incubated at 37°C with 5% CO₂/95% air for 72 hours.

Both Namalwa and Namalwa/MDR1 cells were centrifuged for 10 min at 300 xg at 4°C (Sorvall RC3C centrifuge). The cells were washed with complete medium without FBS and centrifuged again as above. The cells were resuspended in complete medium without FBS at 2×10^5 cells/mL. Just before plating cells, Vincristine was added to the cells to bring to a final concentration of 50 nM. Cells were set aside without Vincristine to be used as a positive control. RTX and UV22-2 were diluted from their stock solutions (13 mg/mL and 5 mg/mL, respectively) in complete medium without FBS to 0.0012- 0.6 mg/mL. Then 100 μ L of these MAb solutions was added to each well of a 96-well tissue culture plate (BD Falcon, San Jose, CA). 100 μ L of complete medium without FBS was used as the negative control. One hundred μ L of the appropriate cell suspension, with or without Vincristine, was added. This gave a final concentration of Vincristine of 25 nM, and MAb concentrations of 0.0006-0.3 mg/mL. Plates were incubated at 37°C with 5% CO₂/95% air for 24 or 48 hours.

After incubation, 10 μ L of [3 H]-thymidine (1 mCi/mL, Amersham Biosciences, Piscataway, NJ), diluted 1:10 in complete medium without FBS was added to each well of cells. The cells were incubated as above for four more hours. They were then harvested onto a FilterMAT (Skatron, Sterling, VA) using a Skatron cell harvester (Skatron, Sterling, VA). FilterMATs were counted using a β -counter (Wallac 1410, Pharmacia/Pfizer, New York, NY). Data were calculated as average counts per minute (cpm) using triplicate wells for each data point. Dose response curves were generated based on expressing cpm from treated cells as a fraction of cpm from untreated cells. The % incorporation of [3 H]-thymidine by treated cells was calculated using the incorporation of non-treated cells as 100%. IC₉₀ values (defined as the concentration of drug that reduced [3 H]-thymidine incorporation by 90%) were determined graphically from relative survival curves. The experiment was repeated 6 times.

Preparation and analysis of lipid rafts for Western Blot.

Namalwa/MDR1 cells were placed in conical tubes (BD Falcon, San Jose, CA) and centrifuged for 10 minutes at 419 x g at 4°C (Sorvall RC3C centrifuge). The cells were washed with complete medium with 10% FBS and centrifuged again as above. The cells were resuspended in complete medium with 10% FBS at 1×10^7 cells/mL and vortexed, and they were divided into 10 mL aliquots in conical tubes (BD Falcon, San Jose, CA). They were then pre-warmed at 37°C for five minutes, rotating (50 Hz) (LabQuake Shaker, Berkeley, CA). MAbs (115 μ L of RTX stock at 13 mg/mL or 203 μ L of UV22-2 stock at 7.4 mg/mL) were added to each aliquot and cells were vortexed to bring the final concentration of antibody to 150 μ g/mL. Untreated aliquots were used as controls. The

cells were incubated for 15, 30, and 60 min at 37°C. Following incubation, cells were centrifuged for 10 min at 419 x g at 4°C (Sorvall RC3C centrifuge) and were washed twice in 15 mL PBS, and the supernatant was discarded. In order to fractionate the cholesterol and sphingolipid-rich membrane microdomains (lipid rafts), the cell pellets, treated and washed as above, were lysed in 1 ml of 2x lysis buffer containing 20 mM Tris and 2% Triton X-100 pH 7.5, supplemented just before use with protease inhibitors (2 µg/ml aprotinin, 2 µg/ml leupeptin, 2 mM Na₂MoO₄, 2 mM Na₃VO₄, and 2 mM PMSF). Lysis buffer was added to the cell pellets, the cells were thoroughly vortexed, incubated on ice for 60 minutes, and then pelleted by centrifugation for 10 minutes at 900 x g at 4 °C (Sorvall RC3C centrifuge) to pellet nuclei and particulate debris. The pellet was removed using a glass Pasteur pipette. One mL of a solution of 85% sucrose in 20 mM Tris buffer (in deionized H₂O, pH adjust to 7.5 with HCl) without Triton X-100 was added to the bottom of a 12 ml ultra-clear ultracentrifuge tube (14 x 85, Beckman, Palo Alto, CA). One mL of the cloudy supernatant (1:1 volume ratio) was added to the bottom of the ultracentrifuge tube and carefully pipetted up and down with a graduated plastic pipette to mix well. Over this layer, 6 ml of 35% sucrose in the same buffer was carefully added with another plastic pipette, so as to maintain the interface. Finally, 3.5 ml of 5% sucrose in the same buffer was layered on top. The tubes were centrifuged for 16-20 h at 4° C at 210,053 x g (Beckman ultracentrifuge, L8-M, using a SW 41 Ti rotor). Twelve fractions of 1 ml each were collected from the top to the bottom of the tube with a 1 mL micropipette, and fractions were placed in 1.5 mL eppendorf tubes for analysis by WB. In some experiments, lipid raft fractions (3-6) and soluble fractions (9-12) were combined into two pools and analyzed by WB. Protein concentration of each fraction and

of pools was determined using BCA™ protein assay and micro Bicinchoninic Acid (BCA)™ protein assay reagent kits from Pierce.

BCA protein assay

The BCA protein assay was performed using either the BCA™ Protein Assay Reagent Kit or the Micro BCA™ Protein Assay Reagent Kit (Pierce Biotechnology, Rockford, IL). The BSA protein standards were prepared from stock solution of bovine serum albumin (BSA) (provided in the kit), diluted in tris buffer. The Microplate procedure detailed in the kit was followed to test the protein concentration of 150 µL of each fraction and each pool of fractions prepared in the lipid rafts procedure above before Western Blot analysis was performed. Samples were read using a spectrometer (SpectraFluor Plus, Tecan, Männedorf, Switzerland).

WB analysis

The 12 fractions collected from the ultracentrifuge tube and the two pools (3-6) (lipid rafts) and (9-12) (soluble fractions) were processed for WB analysis as follows:

Buffers were prepared as instructed in the BioRad Mini-Protean II kit, and all were prepared from reagents purchased from Sigma, St. Louis, MO, unless otherwise noted. They included 10% sodium dodecyl sulfate (SDS) (in deionized H₂O), 10% Ammonium Persulfate (APS) (in deionized H₂O), 10X tris-buffered saline (24g Tris, 87g NaCl, 1 L deionized H₂O, pH adjusted to 7.5 with HCl), 1.5 M Tris (in deionized H₂O, pH adjusted to 8.8 with HCl), 0.5 M Tris (in deionized H₂O, pH adjusted to 6.8 with HCl), 10X electrophoresis stock buffer (30g Tris, 144 g Glycine in 1 L deionized H₂O), Running

buffer (100 mL electrophoresis stock buffer, 10 mL 10% SDS in 890 mL deionized H₂O), Transfer buffer (100 mL electrophoresis stock buffer, 200 mL methanol in 700 mL deionized H₂O), 30% acrylamide/Bis (29.2 g Acrylamide, 0.8 g Bis in 100 mL deionized H₂O), and 2X sample buffer (3.55 mL deionized H₂O, 1.25 mL 0.5 M Tris-HCl, pH 6.8, 2.5 mL glycerol, 2.0 mL 10% SDS, 0.2 mL 0.5% bromophenol blue).

Each fraction prepared in the lipid raft separation was collected in a 12 mL ultracentrifuge tube (Beckman, Palo Alto, CA) and 10 mL of lysis buffer (25 mM MES, pH 6.5, 150 mM NaCl, 1% Triton X-100, all from Sigma, St. Louis, MO) was added. The samples were ultracentrifuged for 1.5 hours at 4° C at 210,053 x g (Beckman ultracentrifuge, L8-M, using a SW 41 Ti rotor). The supernatant was aspirated and discarded.

200 µl from each sample was mixed with 200 µl electrophoresis reducing buffer containing 0.5 M Tris at pH 6.8, 2% SDS, and 5% 2-mercaptoethanol. Samples were boiled for 5 min at 100°C in an oil bath (American Scientific Products, Multi-Blok heater, H2025-1A). Up to 40 µL of each sample was loaded into a well in the appropriate gel. Samples were electrophoresed either on 6% acrylamide gels (for 15 mL gel: 8mL deionized H₂O, 3 mL 30% acrylamide/Bis, 3.8 mL 1.5 M Tris, 0.15 mL 10% SDS, 0.15 mL 10% APS, 0.012 mL TEMED (tetramethylethylenediamine)) to detect of P-gp or on 12 % acrylamide gel (for 15 mL gel: 5 mL H₂O, 6.0 mL 30% Acrylamide/Bis, 3.8 mL 1.5 M Tris, 0.15 mL 10% SDS, 0.15 mL 10% APS, 0.006 mL TEMED) to detect CD20. The gels were transferred to membranes (Immun-Blot PVDF Membrane, Bio-Rad Laboratories, Hercules, CA) according to the BioRad protocol for the Mini Protein II Electrophoresis / Transfer Cells, using 100 volts for 60 minutes. Membranes were treated

with 2% BSA for 2 hours following protein transfer, then mixed with the primary antibody (rabbit anti-MDR 1 $\mu\text{g/mL}$ (Santa Cruz Polyclonal IgG, Santa Cruz, CA, 35 μL in 7 mL TBS/Tween) or anti-CD20 0.5 $\mu\text{g/mL}$ (Santa Cruz Polyclonal IgG, Santa Cruz, CA, 17.5 in 7 mL TBS/Tween)); and incubated overnight at 4°C on a rocker (Rocker II, 260350, Boekel Scientific, Feasterville, PA). Samples were then incubated on a rocker for 1 hour with the appropriate horseradish peroxidase (HRP)-labeled secondary antibody (e.g. HRP-anti-rabbit Ig, Amersham Pharmacia, UK; HRP- anti-mouse Ig, Amersham Pharmacia, UK). The membranes were covered with a chemiluminescence buffer (Amersham Pharmacia) for one minute, then placed in a sample size Ziploc bag and developed on hyperfilm ECI (Amersham Pharmacia, UK) in the dark room using a Kodak m35Ax OMAT Processor. The bands on the WB corresponding to the size of proteins of interest (e.g. 170 kDa for P-gp; 33 - 37 kDa for CD20) were scanned with the Photo suite program (version 4, Platinum, MGI Software Corp/Roxio). The experiment was repeated 8 times.

RESULTS

Namalwa/MDR1 Cells Expressed P-gp and CD20

The expression of P-gp and CD20 on Namalwa/MDR1 and parental Namalwa cells was determined by indirect immunofluorescence staining using the primary antibodies UIC2 (to detect P-gp) and RTX (to detect CD20) and the secondary antibody FITC-GAMIg. Both parental Namalwa and Namalwa/MDR1 cell lines expressed similar levels of CD20 (Table 1).

Cells	Surface Marker	% Positive Cells	MFI*
Namalwa	CD20	94	93
	P-gp	2.1	15
Namalwa/MDR1	CD20	98.1	79
	P-gp	98.6	320

Table 1. The expression of CD20 and P-gp on the surface of Namalwa/MDR1 and parental (MDR1⁻)

Namalwa cells. FACS analysis demonstrated that both Namalwa and Namalwa/MDR1 cell lines expressed similar levels of CD20. 1×10^7 cells/ml were incubated with 100 μ g/ml RTX or UIC2. Only Namalwa/MDR1 cells expressed P-gp (98.6% vs. 2.1% for parental Namalwa cells). *Mean Fluorescence Intensity

CD20 was expressed at a low density on both Namalwa/MDR1 and Namalwa cells (MFI's of 79 and 93 respectively), but, in both cases, greater than 90% of cells were positive. Greater than 95% of the Namalwa/MDR1 cells expressed P-gp (98.6% positive cells), while only 2.1% of the parental Namalwa cells were positive.

In addition, indirect immunofluorescence was used to investigate the expression of P-gp on the surface of Namalwa/MDR1 cells that had been maintained for 8 weeks in culture. After 8 weeks in culture, 83% of the cells expressed P-gp with an MFI of 26. These results suggested that with prolonged culture, the expression of P-gp by Namalwa/MDR1

cells decreased. Therefore we maintained Namalwa/MDR1 cells in culture for 6 weeks, when we thawed a new batch of cells. Hence, while both parental Namalwa cells and Namalwa/MDR1 cells expressed CD20, P-gp was expressed only by the Namalwa/MDR1 cells.

RTX modestly inhibited the growth of both P-gp⁺ and P-gp⁻ cells

To determine the effect of RTX on cell growth, both Namalwa/MDR1 and P-gp⁻ cells (Ramos, parental Namalwa) were cultured in the presence of MAbs, and their viability was determined by trypan blue exclusion. Several concentrations of RTX were used in order to determine the optimal concentrations of the MAb to use in the cytotoxicity experiments. P-gp⁺ and P-gp⁻ cells cultured in medium grew exponentially in culture for 5 days without MAbs (**Figure 3**). When cells were cultured with 100 µg/mL RTX, their growth was modestly inhibited. (~30%) The effect of RTX on tumor cell growth was dose-dependent, with 100 µg/mL, 250 µg/mL, and 500 µg/mL reducing growth by 30%, 50%, and 68%, respectively, after 5 days (data not shown). These results demonstrate that 5 days of incubation with RTX modestly inhibited the growth of tumor cells regardless of whether the cells expressed P-gp on their surface.

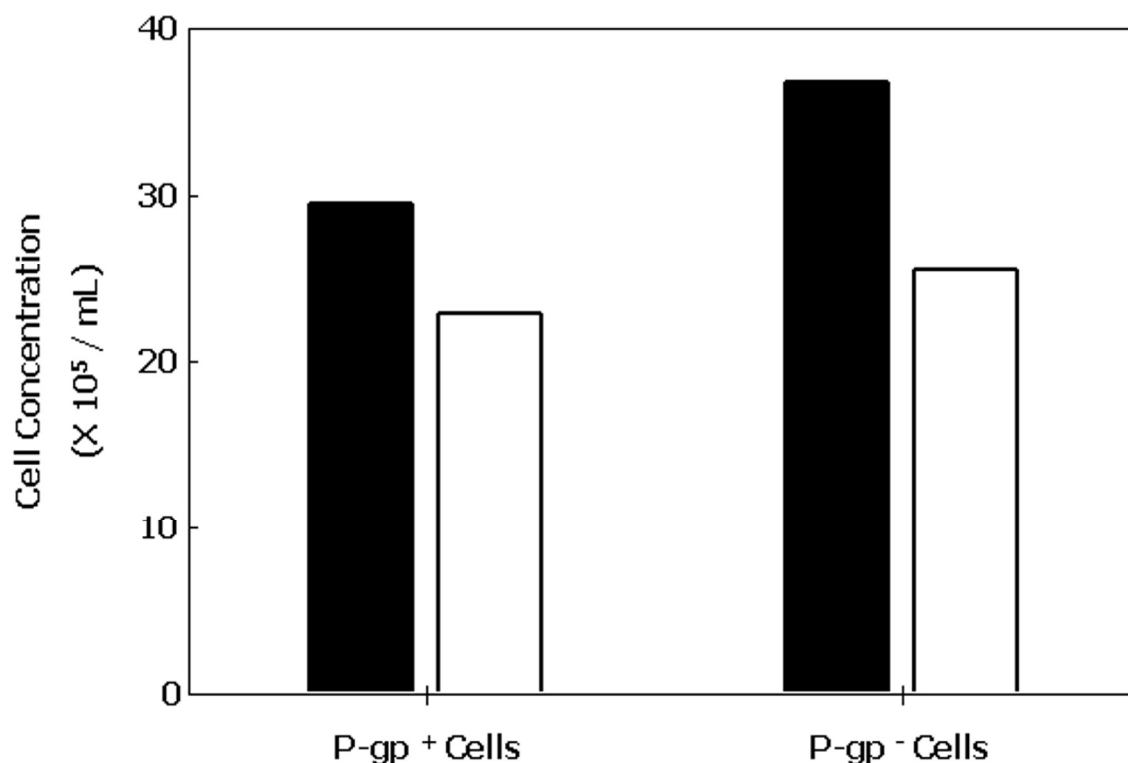


Figure 3. The growth of P-gp⁺ and P-gp⁻ cells cultured with and without RTX. P-gp⁺ and P-gp⁻ cells cultured without MAbs (black bars) grew exponentially in culture for 5 days. When cells were cultured with RTX (white bars) their growth was modestly inhibited. (~30%) The graph is one representative experiment of five experiments performed to determine the optimal concentrations of RTX to use in the cytotoxicity experiments. This is one representative experiment of 2 performed.

RTX chemosensitized Namalwa/MDR1 cells

[³H]-thymidine incorporation was used to determine the effect of RTX on the proliferation of Namalwa and Namalwa/MDR1 cells cultured with chemotherapeutic agents. Both cell lines were cultured with different concentrations of doxorubicin or Vincristine for 72 hours and pulsed with [³H]-thymidine for four hours. As shown in **Figure 4A**, the parental Namalwa cells were killed by incubation with doxorubicin alone (IC₉₀ of 5.5 nM). The presence of RTX had no effect on the cytotoxicity of doxorubicin on the P-gp⁻ cells. Incubation with doxorubicin alone was much less effective in killing

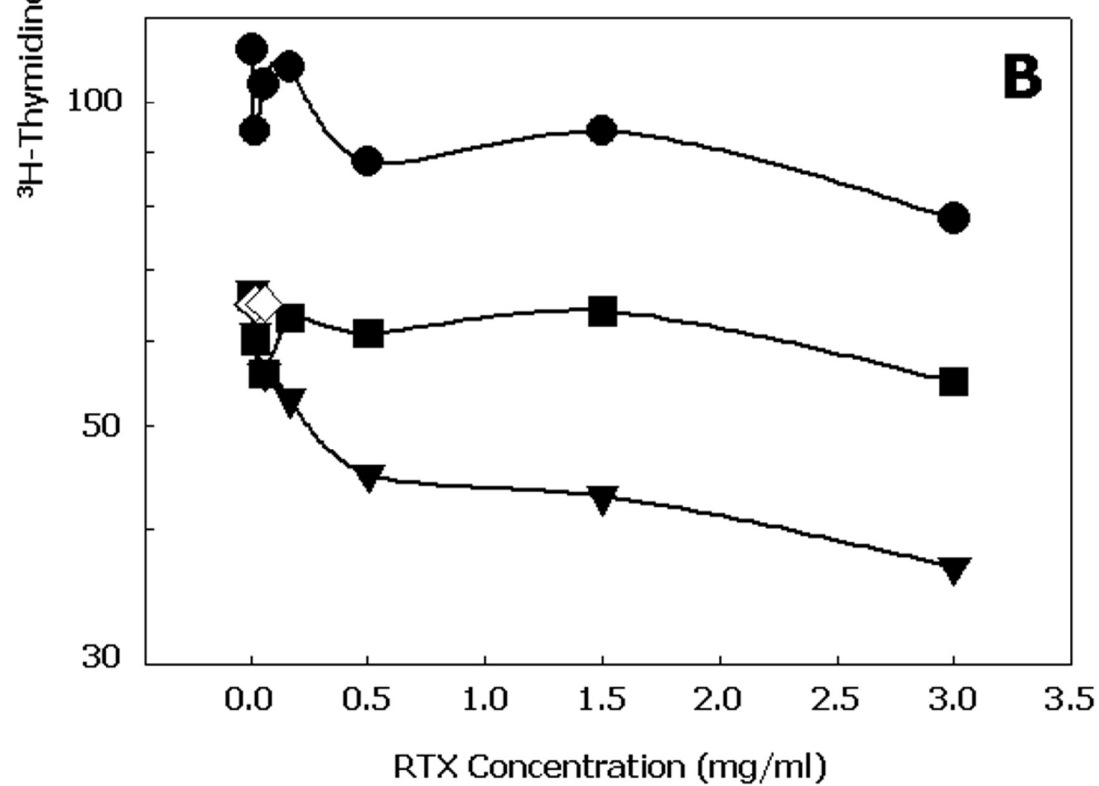
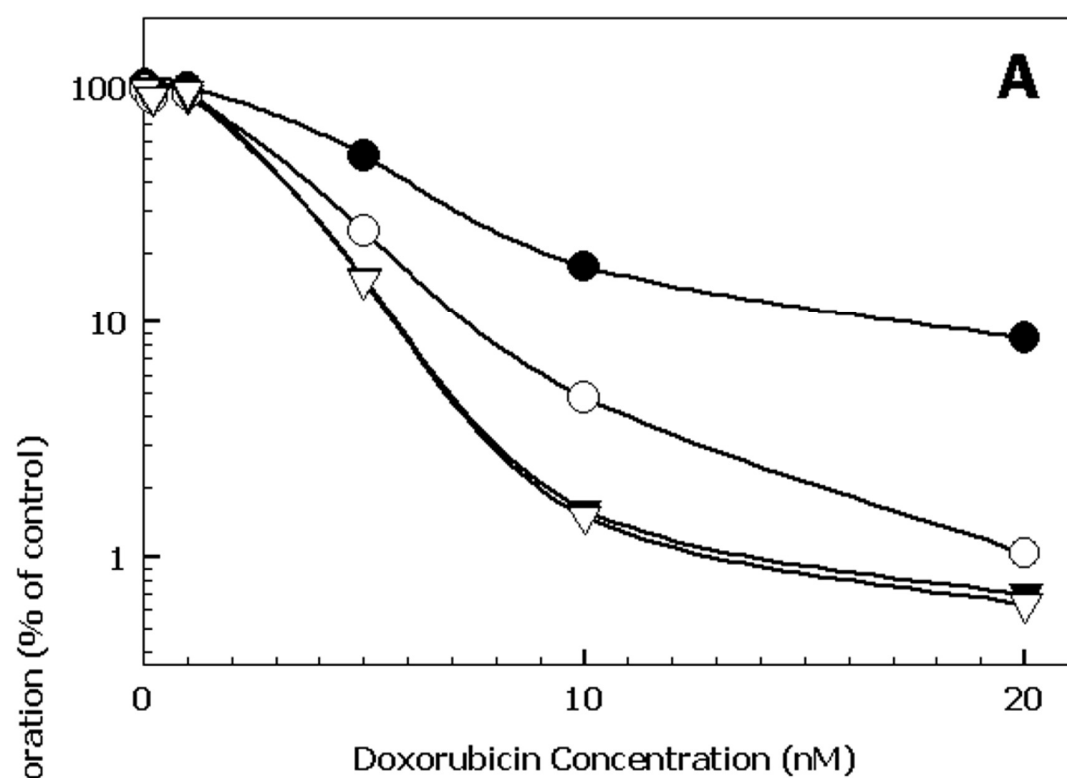
Namalwa/MDR1 cells (IC_{90} of 17.5 nM). However, when the Namalwa/MDR1 cells were incubated with RTX plus doxorubicin, the IC_{90} of doxorubicin decreased to the level observed in Namalwa cells (7.5 nM). Therefore, RTX chemosensitized P-gp⁺ cells to doxorubicin.

As shown in **Figure 4B**, RTX alone had little cytotoxicity with the Namalwa/MDR1 cells over the 72 hour incubation period. When the killing assay was performed in the presence of 25nM Vincristine, a steady cytotoxic effect was observed in Namalwa/MDR1 cells. However, adding different concentrations of RTX to the Vincristine in the same assay demonstrated that the cytotoxic effect of vincristine increased proportionally with the concentration of RTX. No increase in cytotoxic activity was observed when UV22, an anti-CD22 MAb, was used with Vincristine. From these results, it can be concluded that RTX and Vincristine together were more effective in killing P-gp⁺ cells than either agent alone, and that this synergy did not occur when a reactive but unrelated MAb was used. Together, the cytotoxicity experiments demonstrate that RTX chemosensitizes Namalwa/MDR1 cells.

Figure 4. The cytotoxic effect of RTX on P-gp⁺ and P-gp⁻ Namalwa cells. Cells were incubated at 1.2×10^5 /well in 96-well microtiter plates for 72 hours at 37°C, followed by a 4-hour pulse with [³H]-Thymidine.

A. [³H]-Thymidine incorporation in Namalwa cells: P-gp⁺ cells incubated with doxorubicin (●) doxorubicin + RTX (10^{-7} M)(○) and P-gp⁻ cells incubated with doxorubicin (▼) doxorubicin + RTX (10^{-7} M) (▽) This was one representative experiment of 3 performed.

B. [³H]-Thymidine incorporation in P-gp⁺ Namalwa cells incubated as described above with different concentrations of RTX (●); RTX + Vincristine (25 nM) (constant concentration)(▼); different concentrations of an anti-CD22 MAb (UV22) + Vincristine (25 nM) (■); Vincristine (25 nM) alone (◇). This was one representative experiment of 2 performed.



RTX inhibited the cellular efflux of Rhodamine-123 as effectively as Verapamil

It was hypothesized that RTX chemosensitized P-gp⁺ cells by blocking the action of the P-gp pump. A Rhodamine-123 efflux assay was therefore used to determine the activity of the P-gp pump in the cell membrane of Namalwa/MDR1 cells (**Figure 5**). The effect of RTX on the activity of the pump was compared to the effect of Verapamil. Verapamil is a drug known to inhibit the activity of the P-gp pump. [70] The cells were incubated with Rhodamine-123, washed, and the efflux of the dye was determined.

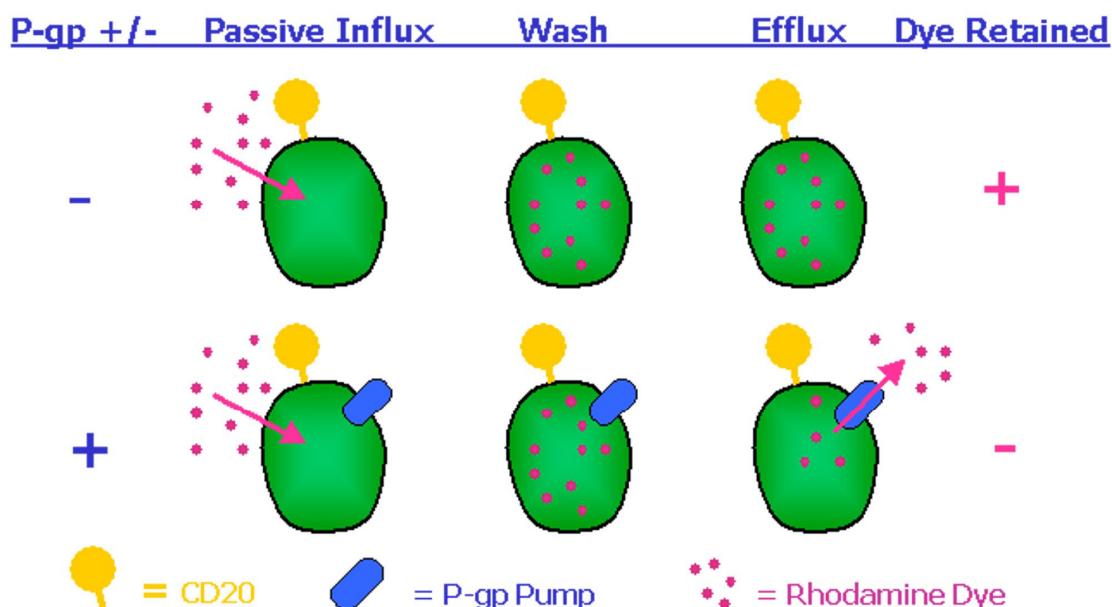


Figure 5. The Rhodamine-123 dye efflux assay to measure P-gp activity. The assay was used to assess the efflux of Rhodamine-123 by the P-gp pump. In cells that did not express P-gp, the Rhodamine-123 dye diffused into the cell and remained. Rhodamine-123⁺ cells were detected on the FACS. When cells expressed P-gp, the dye diffused into the cell, but it was then actively pumped out by the P-gp pump. Hence, the dye was not detected in the cells by FACS analysis. In the presence of an inhibitor of P-gp, in this case Verapamil, the dye did not efflux, and Rhodamine⁺ cells were detected by FACS analysis. We used this assay to test the effect of RTX vs. Verapamil on the activity of the P-gp pump.

Namalwa/MDR1 cells effluxed Rhodamine-123 (**Figure 6**), whereas the parental P-gp⁻ Namalwa cells retained the dye (data not shown). Incubation of Namalwa/MDR1 cells

with Verapamil at 10 μ M blocked the activity of the P-gp pump and the cells retained Rhodamine-123 (**Figure 6**). Incubation with RTX at 10^{-7} M inhibited the activity of the P-gp pump such that the Namalwa/MDR1 cells retained Rhodamine-123. In addition, an anti-CD22 MAb (RFB4) had no effect on the efflux of Rhodamine-123 (data not shown). These data indicate that RTX inhibited the activity of the P-gp pump as effectively as did the well-known P-gp inhibitor, Verapamil.

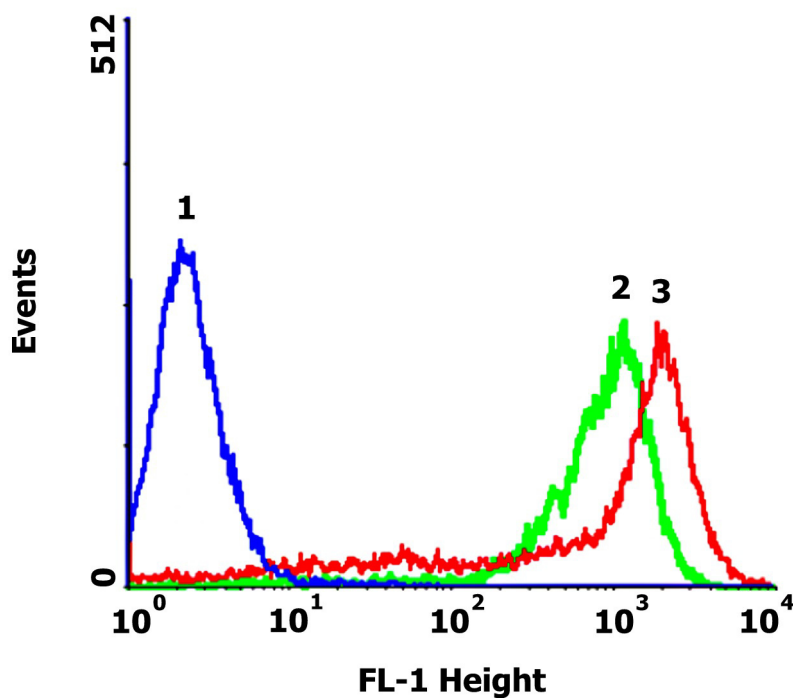


Figure 6. The effect of RTX on P-gp-mediated Rhodamine-123 efflux by MDR1 cells. 5×10^5 / ml Namalwa/MDR1 cells were incubated for one hour at 37° C with 3 μ M Rhodamine-123 alone or in combination with the other reagents as indicated. Cells in media (1); Verapamil (10 μ M) (2); 10^{-7} M RTX (3). Cells were washed twice with RPMI-1640 without FBS, resuspended in FBS-free medium, and incubated for 2 hours at 37°C to measure the efflux of Rhodamine-123. This is one representative experiment of 10-15 performed.

RTX induced the translocation of P-gp out of lipid rafts

After previous experiments demonstrated that RTX chemosensitized Namalwa/MDR1 cells and inhibited the activity of the P-gp pump, a possible mechanism for the action of RTX was sought. It had been postulated that the lipid phase of the plasma membrane is important for the activity of P-gp. [24] Experiments with an anti-CD19 MAb indicated that in Namalwa/MDR1 cells cultured without MAbs and then lysed, ~40% of the P-gp was located in lipid rafts, while the other 60% was located in the soluble fraction of the membrane following cell lysis. [68] It had been shown previously that following sucrose gradient ultracentrifugation of the cell lysates, lipid rafts were present in fractions 3-6 and the detergent-soluble fraction of the membrane was present in fractions 9-12. Therefore, this method of separating rafts from the soluble fraction of the cell membrane was used to follow the proportion of CD20 and P-gp in the lipid rafts vs. the soluble fraction of the membrane (**Figure 7**).

Other detergents have been used to separate rafts from non-rafts by other investigators. [60] [47] Each detergent, and even a different concentration of the same detergent, generated a slightly different pattern of protein partitioning in raft and non-raft fractions. Though several detergents have been used to study the position of CD20 in the membrane, the standard in the field continues to be Triton-X. Recently, detergent-free methods of separating rafts from non-rafts have been introduced and refined. [71-73] These methods involved mechanical disruption of membranes by sonication and/or shearing resulting in protein partitioning between rafts and non-rafts. This partitioning is similar to that found in detergent-dependent protocols for raft isolation, but theoretically eliminated the detergent-dependent variability of those methods. However, detergent-free

methods have their own problems, including low yield and potential disruption and mixing of membrane lipids. There was also some variability in protein partitioning based upon duration of sonication. None of these detergent-free methods has been applied to CD20 research, but this could potentially be a useful tool for carrying out functional assays that are detergent-sensitive. For our experiments, Triton X was chosen because it is the standard method in the field.

Following ultracentrifugation of the cell lysates, fractions were electrophoresed and WBs were carried out with the relevant or control MAbs (**Figure 8, A and B**). When MDR cells were cultured in medium, a significant proportion of P-gp was found in the raft fractions. Following incubation of the cells with 150 µg/mL RTX, the P-gp molecules present in lipid rafts translocated into the soluble fraction of the membrane. Culturing cells with an anti-CD22 MAb had no effect. Translocation was rapid and occurred after exposing the cells to RTX for 15 min. From these experiments, it can be concluded that RTX induced P-gp to translocate out of lipid rafts and into the detergent-soluble fraction of the cell membrane.

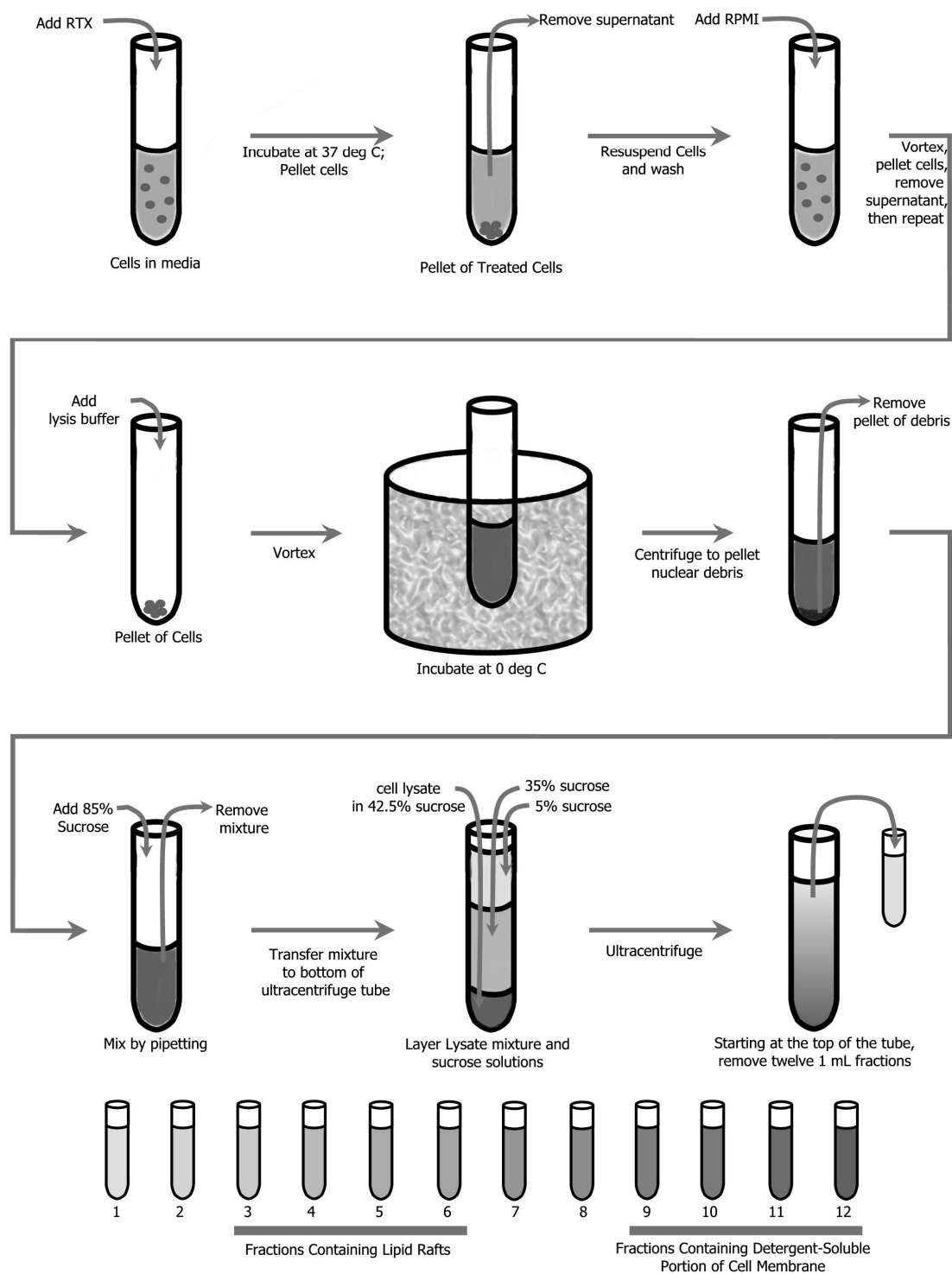


Figure 7. Preparation of Lipid Rafts for WB Analysis. Namalwa/MDR1 cells were incubated with MAbs (at 10^{-7} M / 10^6 cells for one hour at 37° C), then washed twice with RPMI, pelleted and lysed on ice

for one hour with lysis buffer containing 20 mM Tris, 2% Triton X-100 pH 7.5, 2 µg/ml aprotinin, 2 µg/ml leupeptin, 2 mM Na₂MoO₄, 2 mM Na₃VO₄, and 2 mM PMSF. The cell lysate was ultracentrifuged at 210,053 x g through a sucrose gradient (5 – 42.5%) for 16-20 hours at 4° C and twelve fractions of one ml were collected from the top to the bottom of the tube. Individual fractions or pooled fractions were analyzed by WB as indicated.

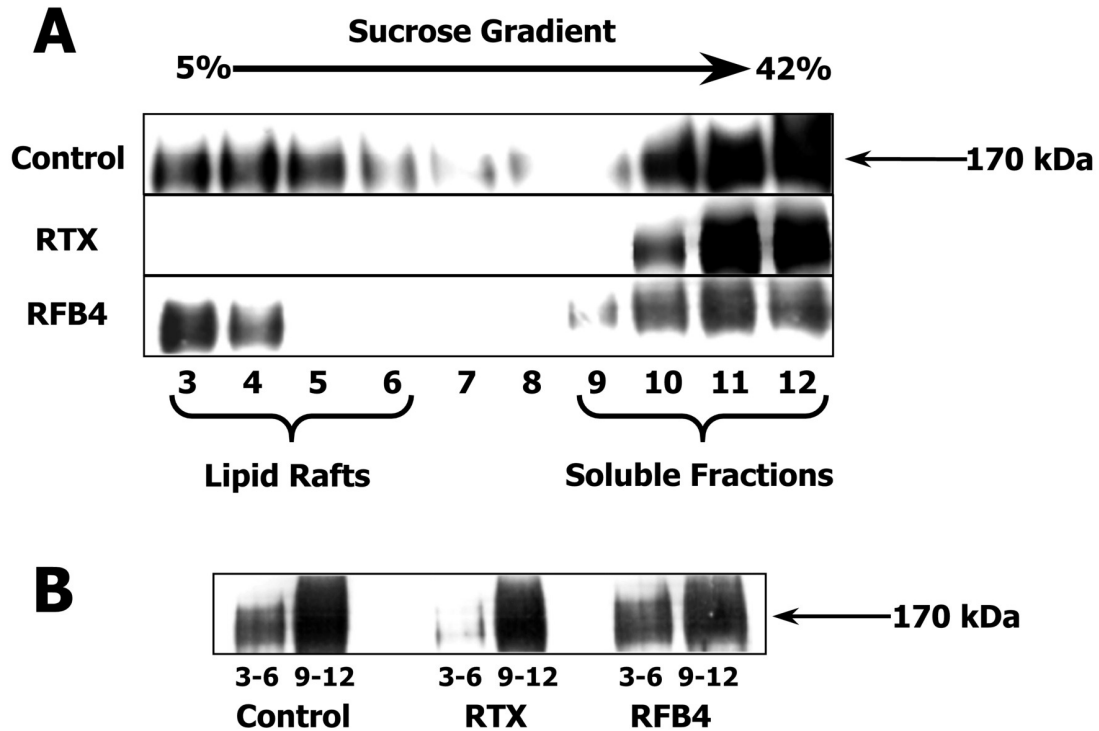


Figure 8. WB analysis of the distribution of P-gp in lipid rafts in Namalwa / MDR1 cells before and after incubation with MAbs.

A. The distribution of P-gp in the 12 fractions separated on sucrose gradients before and after incubation of cells with MAbs followed by cell lysis. This is one representative experiment of 5-7 performed.

B. The distribution of P-gp in the pools of fractions, 3-6 (lipid rafts), and 9-12 (soluble fraction). This is one representative experiment of 5-7 performed.

RTX induced the translocation of CD20 into lipid rafts

WBs were also used to follow the location of CD20 in the cell membrane after incubation of the cells with RTX. In Namalwa/MDR1 cells cultured without MABs, virtually all the CD20 was present in the soluble membrane fraction (**Figure 9, A and B**). Following incubation with RTX, a significant portion (but not all) of the CD20 molecules translocated into lipid rafts. In contrast, incubation with an anti-CD22 antibody did not alter the distribution of CD20 in the membrane. These results suggest that the translocation of CD20 out of the detergent-soluble fraction of the membrane and into lipid rafts took place concurrently with the translocation of P-gp out of lipid rafts.

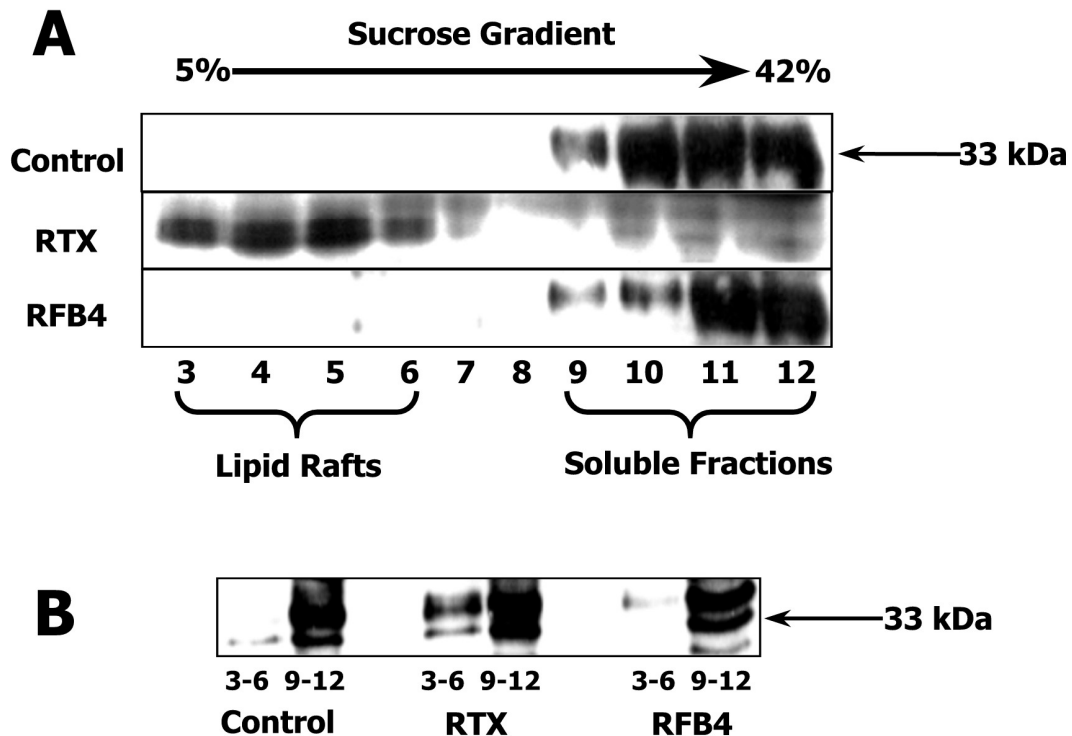


Figure 9. WB analysis of the distribution of CD20 in lipid rafts in Namalwa/MDR1 cells before and after incubation with MABs

A. The distribution of CD20 in the 12 fractions separated on sucrose gradients before and after incubation of the cells with MAbs followed by cell lysis. This is one representative experiment of 5-7 performed.

B. The distribution of CD20 in the pools of fractions, 3-6 (lipid rafts), and 9-12 (soluble fraction). This is one representative experiment of 5-7 performed.

DISCUSSION

General

There is still no cure for NHL, and treatments that currently prolong life have severe adverse effects and can become ineffective following the development of MDR. Targeted therapies that will minimize damage to healthy cells and eliminate malignant ones are needed. Targeted therapies to overcome MDR are similarly lacking. MAbs represent a major advance in effectively treating many cancers, including NHL. RTX, in particular, has induced lasting remissions in patients as a single agent and when combined with chemotherapeutic drugs, and it has chemosensitized MDR cells *in vitro*. Understanding the mechanism of action of RTX in chemosensitizing MDR cells would provide valuable insights into future drug design and therapy.

Objectives and Major Findings

The objectives of this study were as follows: 1) to confirm that Namalwa/MDR1 cells express P-gp and CD20 and to determine whether expression changes after time in culture, 2) to determine the effect of RTX on the growth of Namalwa/MDR1 and parental Namalwa cells, 3) to determine the cytotoxic effect of RTX plus chemotherapy on Namalwa/MDR1 cells, 4) to determine the effect of RTX on the activity of the P-gp pump, 5) to determine whether RTX altered the membrane distribution of P-gp such that it could no longer function as an active pump. To this end, we studied the distribution of P-gp and CD20 in lipid rafts vs. the soluble fraction of the cell membrane before and after treatment of MDR1 cells with RTX.

The major findings to emerge from this study were as follows: 1) We confirmed that Namalwa/MDR1 cells expressed P-gp and CD20, and that expression of P-gp changed with time in culture; 2) RTX modestly inhibited the growth of both Namalwa/MDR1 and parental Namalwa cells; 3) RTX chemosensitized Namalwa/MDR1 cells; 4) RTX inhibited the activity of the P-gp pump; 5) RTX induced the translocation of P-gp out of lipid rafts and the translocation of CD20 into lipid rafts.

RTX modestly inhibited the growth of P-gp⁺ and P-gp⁻ B-NHL cells *in vitro*

In this study, *in vitro* culture with 100 µg/mL RTX modestly inhibited the growth of Namalwa/MDR1 cells, parental (P-gp⁻) Namalwa cells, and Ramos (P-gp⁻) cells.

Additional experiments showed that growth inhibition of Namalwa/MDR1 cells by RTX was dose-dependent. These results suggested that the modest anti-proliferative effects of RTX *in vitro* were not mediated by ADCC or CDC and that this anti-proliferative effect was not affected by the expression of P-gp.

The hypothesis that the anti-tumor activity of RTX and other anti-CD20 MAbs resulted from direct effects on the ligation of CD20 was demonstrated in experiments using several B-NHL cell lines. The mechanism(s) responsible for these direct effects were debated in the literature, and they included inhibition of DNA synthesis, cell cycle arrest, translocation of phosphatidylserine to the outer membrane, induction of apoptosis, activation of serine/threonine protein tyrosine kinases, caspase activation, increased intracellular calcium and down-regulation of anti-apoptotic proteins. [74] Recently, Bezombes et al. proposed that it is the direct anti-proliferative effect of RTX that was primarily responsible for its *in vivo* anti-tumor effect. [75] The authors demonstrated that

Daudi cells (P-gp⁻ Burkitt's lymphoma) treated with 10 µg/mL RTX exhibited growth inhibition, arrest of cells in G₁ phase, and loss of clonogenic potential but did not undergo apoptosis. The mechanism proposed by the authors for this anti-proliferative effect involved activation of acid sphingomyelinases and a ceramide-triggered signaling pathway. The most striking effect of treatment with RTX that we observed, chemosensitization of Namalwa/MDR1 cells by inactivation of the P-gp pump, was not evident in our growth inhibition experiments with Namalwa and Namalwa/MDR1 cells. The effect of anti-sphingomyelinase was tested in Namalwa/MDR1 cells in combination with RTX treatment to determine if the reversal of MDR would be affected by blocking the acid sphingomyelinase pathway. Neither the chemosensitization nor the inactivation of P-gp by RTX were altered (data not shown). Rose et al. demonstrated that in P-gp⁻ human B-NHL cell lines, RTX had an *in vitro*, dose-dependent anti-proliferative effect that was synergistic with a similar effect mediated by glucocorticoids. [76] The authors demonstrated that incubation of cells with RTX resulted in significant dose-dependent growth inhibition in 7 of 9 cell lines tested (Daudi, Ramos, DHL-4, Granta 519, NCEB-1, OCI Ly8, and Tab). The mean percentage of growth inhibition at a dose 10 µg/mL of RTX ranged from 18% to 83%. A previous study by Ghetie et al. [28] investigated the *in vitro* anti-proliferative effect of RTX monomers (1-100 µg/mL) or homodimers on P-gp⁻ DHL-4 and Ramos cells. The experiments demonstrated a modest anti-proliferative effect of RTX monomers, and a greater anti-proliferative effect of homodimers of RTX on both cell lines. Several other studies demonstrated similar inhibition of B-NHL cell growth by anti-CD20 MAbs, [77, 78] though none directly compared the anti-proliferative effects of RTX on P-gp⁺ and P-gp⁻ cell lines. Experiments using RTX or other anti-CD20 MAbs

may have used antibody preparations containing homodimers, and these dimers may have been partially responsible for the more substantial anti-proliferative effect of RTX that was observed with some cell lines.

The goal of our investigation of the anti-proliferative effect of RTX on Namalwa and Namalwa/MDR1 cells was to determine what that effect was and whether it changed based on the presence or absence of P-gp expression by the cell. RTX exerted an anti-proliferative effect on B-NHL cells *in vitro*, and in our studies, this effect did not vary with the expression of P-gp on the cells.

RTX Chemosensitized Namalwa/MDR1 Cells

In this study, incubation with RTX chemosensitized Namalwa/MDR1 cells to Vincristine and doxorubicin. In the absence of RTX, these cells were resistant to killing by these chemotherapeutic agents, but when RTX was added, the cells became as sensitive to killing as the parental, P-gp⁻, Namalwa cells.

The debate over the mechanisms of chemosensitization by RTX continues in the literature. NHL B cell lines were studied and shown to be chemosensitized to many chemotherapeutic agents by treatment with RTX, even when those cells did not express P-gp. [37] The binding of RTX to CD20 on the B cell affects several signaling pathways mediated by CD20, and these pathways were shown to intersect those utilized by chemotherapeutic agents. [79] Several studies proposed that RTX chemosensitized P-gp⁻ cells that were resistant to chemotherapeutic agents by inhibiting anti-apoptotic pathways that were constitutively activated in the cancer cells. These anti-apoptotic pathways protected cancer cells from drug-induced apoptosis by various mechanisms. It was shown that when RTX bound to CD20 on the surface of the B cell, CD20 translocated into lipid

rafts and there it was associated with the Src family of tyrosine kinases. [80, 81] The resultant activity of these Src kinases was linked with down-regulation of the expression of Bcl-2 and inhibition of Bcl-xL, two anti-apoptotic proteins that were over-expressed in many cancers, including NHL. These proteins acted by inhibiting the release of cytochrome c from mitochondria, thus halted the activation of caspases (3, 8, 9) that would lead to apoptosis. [79] The details of these pathways continue to be investigated. The intracellular signaling pathways affected by RTX addressed chemosensitization of NHL cells in the absence of P-gp. P-gp was an important component of MDR that was not linked with these pathways. It is possible that the chemosensitization observed in our studies is due, in part, to an effect of RTX on these signaling pathways. We found that RTX chemosensitized Namalwa/MDR1 cells such that they were killed by chemotherapeutic agents as efficiently as the P-gp⁻ parental Namalwa cells. In addition, RTX had no effect on the killing of parental Namalwa cells. These results suggested that in this cell line, resistance was primarily mediated by the P-gp pump and that the effect of the pump was inhibited by RTX. It is possible that the signaling events described in P-gp⁻ cells involve intracellular pathways that were also involved in the chemosensitization of P-gp⁺ cells. This remains to be explored.

RTX Inhibited the Activity of the P-gp Pump

RTX inhibited the activity of the P-gp pump *in vitro* as effectively as the well-known P-gp inhibitor, Verapamil. Hence, Namalwa/MDR1 cells did not efflux Rhodamine-123 after treatment with RTX. Additional experiments were conducted with other anti-CD20 MAbs, 1F5, 2H7, and B1. [82] None of these MAbs inhibited the activity of P-gp, even

though they did bind to the cells and cross-link their target antigens. In addition, all had similar Kds, and one of the MAbs, B1, cross-blocked the binding of RTX to cells. Even so, none had any effect on the activity of the P-gp pump. Other reports demonstrated that RTX can chemosensitize NHL cells, but there were no reports of its activity on the P-gp pump. [79] Another MAb, anti-CD19 or HD37, was reported to block P-gp activity. [67] The implications of a non-toxic modulator of P-gp activity are important.

There are toxicities associated with the use of virtually all P-gp inhibitors resulting in damage to normal cells in the heart, kidney, brain, intestine, liver, etc. In addition there can be toxicities related to the altered pharmacokinetics of chemotherapeutic agents that cannot be cleared efficiently from the body. The most recent generation of MDR modulators, which included derivatives of Cyclosporine A as well as novel compounds with greater activity against the P-gp pump and less toxicity, have not yet been successful in clinical trials. [83] Using a MAb that was directed only against cells that express CD20 on their surface (normal and malignant B cells, but not including hematopoietic stem cells or plasma cells) eliminates its side effects in other normal tissues. In addition, because resistant cells became chemosensitized, there would be no need for the higher dosages and more aggressive regimens of chemotherapeutic agents often employed in patients with relapsed or refractory lymphomas.

The synergy of RTX with chemotherapy was initially observed in relapsed NHL patients who responded to a combination of RTX and the cyclophosphamide, doxorubicin, vincristine, prednisone (CHOP) regimen. [32] It is conceivable that this synergy could be due, at least in part, to the effect of RTX on cells in the tumor that have up-regulated P-gp after initial rounds of chemotherapy. The use of RTX in both newly diagnosed and

relapsed patients may prevent selection of such P-gp-expressing cell clones and chemosensitize those that are already present.

RTX induced the translocation of P-gp out of lipid rafts and the translocation of CD20 into lipid rafts

Incubation of Namalwa/MDR1 cells with RTX induced the translocation of CD20 into lipid rafts and induced the translocation of P-gp out of rafts. CD20 was localized to the lipid rafts fraction of the cell membrane after treatment with anti-CD20 MAbs, including RTX. [57] In contrast, prior to incubation with MAbs, most of the CD20 molecules were not present in rafts. This translocation was not dependent on the activity of kinases, the supply of ATP, the integrity of the cytoskeleton, or hypercrosslinking of the MAb. [60, 84] Some experiments using different methods of isolating the lipid rafts from the rest of the membrane argued that the localization of CD20 in the membrane is dependent upon which detergent was used to solubilize the membrane. [47]. Hence, other investigators have found that CD20 was present in lipid rafts prior to treatment with MAb when detergents other than Triton X-100 were used, and they suggested that MAb treatment strengthened the constitutive association between CD20 and rafts rather than actively translocating CD20 into rafts. [60] Treatment with MAb, specifically RTX, altered the association between CD20 and lipid rafts, possibly by inducing a physical translocation into rafts which then caused a change in its conformation such that it is less soluble in detergent. Although this might indeed be the case, the use of Triton X to operationally define the effects of RTX on the presence or absence of CD20 in rafts is still meaningful with regard to possible changes in its function and interaction with other membrane

molecules following antibody treatment. CD20 functioned in the cell membrane as a store-operated calcium channel (SOCC), regulating the flux of calcium through the cell membrane based upon the status of intracellular calcium stores. [47] Its activity as a Ca^{2+} channel was altered by its association with lipid rafts. When the residues in the CD20 protein necessary for raft association were deleted, calcium influx across the membrane decreased. [47] This alteration in the activity of CD20 based upon its location in rafts was further investigated by manipulation of the cholesterol content of rafts. Unruh et al [85] demonstrated a decrease in RTX-induced calcium mobilization and apoptosis in B cells after removal of cholesterol with methyl beta cyclodextrin ($\text{M}\beta\text{CD}$). RTX induced resistance to solubilization of CD20 by Triton X-100, but this effect was diminished with cholesterol removal by $\text{M}\beta\text{CD}$. Janas et al [86] reported similar findings. Removal of cholesterol from the cell membrane may have influenced the conformation of CD20 in the cell membrane. For example, Polyak et al [87] noted that the anti-CD20 MAb, FMC7, bound to an epitope on B cells that was sensitive to the cholesterol content of the membrane. Depletion of cholesterol decreased the binding of this MAb, while restoration of cholesterol restored binding. Both the function of CD20 as an SOCC and the RTX-mediated translocation of CD20 into lipid rafts were sensitive to the microenvironment of CD20 in the cell membrane. Changes in rafts affected CD20, and binding of RTX to CD20 also affected rafts.

Different anti-CD20 MAbs demonstrated differing abilities to effect translocation of CD20 into lipid rafts. 1F5 and RTX translocated CD20 into rafts with or without antibody hyper crosslinking. B1 did not translocate CD20 into lipid rafts. [84] We confirmed these results, and another anti-CD20 MAb, 2H7, was also shown to translocate

CD20 into rafts. Interestingly, B1 cross-blocked RTX, suggesting that they both bound to the same or spatially close epitope on CD20 yet B1 did not induce translocation of CD20 into rafts. The significance of the ability of a given MAb to translocate CD20 into lipid rafts is still under investigation. It was proposed that this translocation correlated with the ability of the MAbs to activate complement. [84] From our work, the translocation of CD20 into rafts by RTX did not distinguish RTX from several other anti-CD20 MAbs. However, of the tested MAbs, only RTX translocated P-gp out of lipid rafts, and only RTX inactivated P-gp. [82]

The relationship of P-gp to lipid rafts is complex and not yet fully understood. Bacso et al. [62] investigated the association of P-gp with lipid rafts and the cytoskeleton in colon carcinoma cells and fibroblasts transfected with *MDR1*. One third of P-gp was associated to the cytoskeleton *via* lipid rafts, while 15% was directly associated with the cytoskeleton. The activity of P-gp was limited when cells were depleted of cholesterol with M β CD. [62] In a review of the effects of lipids on P-gp, [24] the authors noted that the removal of lipids associated with P-gp during its purification was associated with its total loss of activity, as measured by ATP hydrolysis capacity. In addition, P-gp was sensitive to the physical state of surrounding lipids, although reports concerning the ideal phase of lipids (gel or liquid crystal) to produce P-gp activity were conflicting. [24] The activity of P-gp was dependent upon its microenvironment in the plasma membrane, and perturbations of that environment decreased both the ATPase activity of the pump and drug binding. Because ~40% of P-gp was present in lipid rafts [61] we hypothesized that the P-gp molecules in rafts were the “active” molecules while those in the soluble membrane fraction were inactive.

P-gp was not only affected by its lipid environment in the membrane, but according to the literature, it also affected the lipids around it. Whether P-gp transported natural long-chain lipids from the inner to the outer leaflet of the membrane continued to be debated in the literature. [24] Studies demonstrated it was a broad-specificity transporter of short-chain lipid analogues, and some suggested that it was involved in sterol transport from the plasma membrane to the endoplasmic reticulum, and thereby controlled cholesterol esterification and biosynthesis in cells. In addition, it was suggested that P-gp transports short-chain analogs of sphingomyelin and glucosylceramides, components of lipid rafts. [24]

Because the activity of P-gp was so sensitive to its lipid environment, it was possible that alterations in cholesterol levels were responsible for the chemosensitization observed after treatment with RTX. In experiments performed by Ghetie et al, incubation of cells with M β CD to remove cholesterol from the membrane did decrease the activity of P-gp (data not shown). [82] However, this effect did not approach the level of chemosensitization caused by incubation with RTX. In addition, treatment of cells with M β CD did not affect the ability of RTX to chemosensitize the cells. This would suggest that chemosensitization by RTX worked via a mechanism independent of alterations in the lipid environment.

Experiments performed in our laboratory suggest that there was no direct association between P-gp and CD20 in the cell membrane of Namalwa/MDR1 cells. [82] Co-precipitation experiments did show that P-gp and CD20 resided in the same membrane patches on the cell surface. However, this finding was not confirmed by Ghetie et al using Fluorescence Resonance Energy Transfer (FRET) analysis, using PE-anti-P-gp as

the donor dye and Cy5-anti-CD20 as the acceptor dye (data not shown). This could have been due to a distance larger than 100 Å between the two molecules on the cell surface resulting in their failure to transfer energy. It could also have been due to the fact that the interaction was weak (as was the case with the interaction between P-gp and CD19). However, if we assumed that there was no direct contact between the two molecules, several other possibilities existed to explain their interaction. **(Figure 10)**

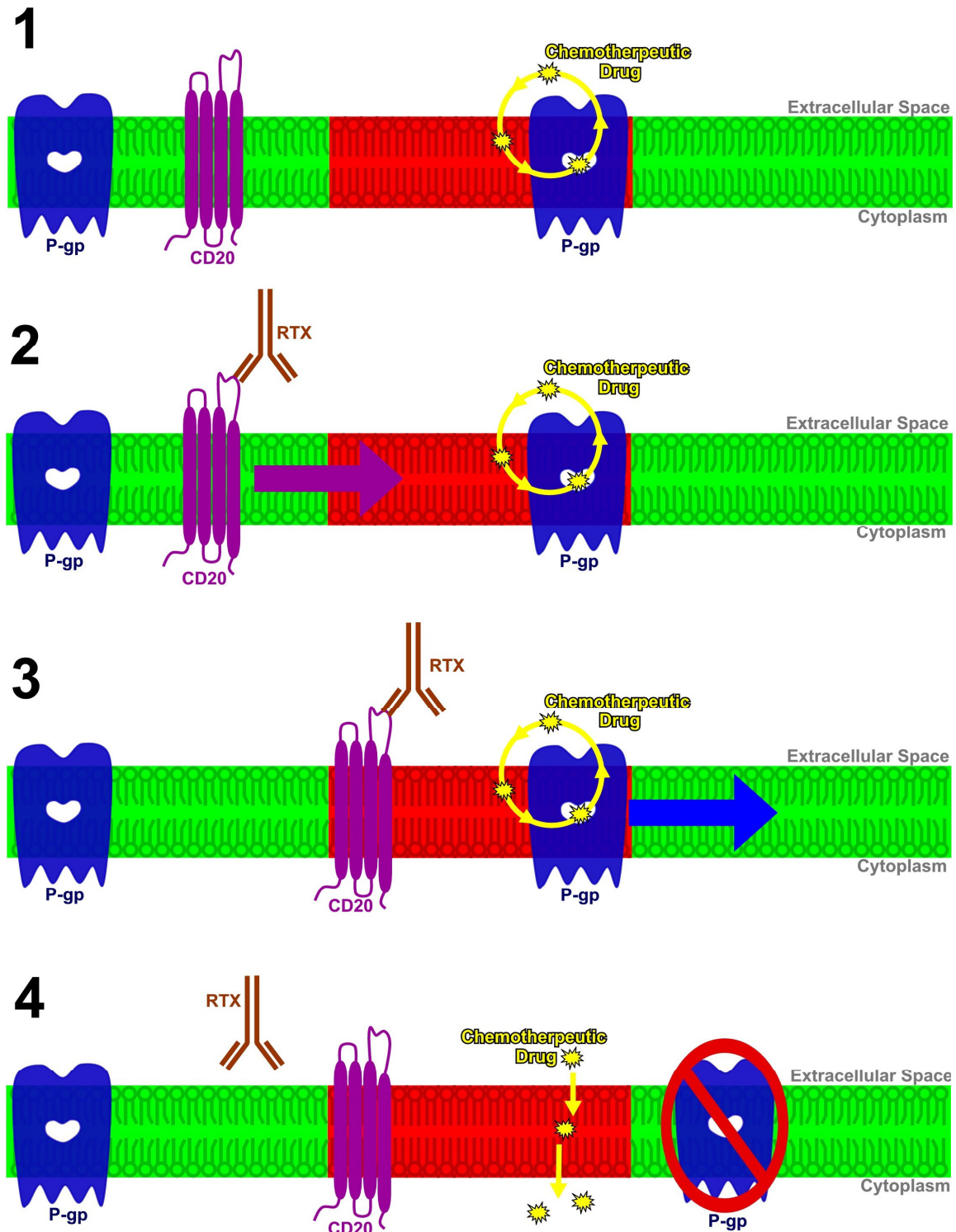


Figure 10. Model of the effect of RTX binding to CD20 on P-gp and lipid rafts. Red represents lipid rafts, while green represents the detergent-soluble remainder of the cell membrane of a Namalwa/MDR1 cell. 1. Prior to exposure to RTX, CD20 resided in the detergent-soluble portion of the membrane.

Approximately 40% of P-gp resided in lipid rafts. These P-gp molecules were actively pumping chemotherapeutic drugs out of the cell, making the cell drug-resistant. Inactive P-gp molecules resided in the detergent-soluble portion of the membrane. 2. RTX bound to CD20 and caused it to translocate from the detergent-soluble portion of the membrane into lipid rafts. 3. P-gp translocated out of lipid rafts. 4. P-gp was inactivated, reversing MDR by allowing chemotherapeutic drugs to accumulate within the cell.

Indirect effects of the interaction between RTX and CD20 may have been responsible for the effect on P-gp. The literature demonstrated that CD20 was associated with several proteins in the membrane, and it was possible that one of these was associated with P-gp. The B cell antigen-specific receptor (BCR) was functionally associated with lipid rafts and CD20 in the cell membrane. A transient association between the BCR and CD20 was evident by immunofluorescence confocal microscopy after B lymphoma cells were incubated with anti-CD20 MAb. [58] The molecules dissociated upon stimulation, but prior to internalization, of the BCR. A further association was inferred from experiments showing that the CD20 molecule became more accessible to binding by anti-CD20 MAbs on the surface of Burkitt's lymphoma cells after engagement of the BCR. [88] The signaling function of the BCR was reported to be enhanced by co-ligation of CD19/CD21 and the BCR. [58] These indirect interactions between CD20 and the BCR suggested that it was possible for binding of anti-CD20 MAbs to specific epitopes on CD20 to affect P-gp by either interfering with the ability of these molecules to interact with P-gp or by altering molecular cross-talk within the lipid raft by some as yet undefined mechanism.

The binding of CD20 by RTX changed the interaction between CD20 and lipid rafts. Perhaps the interaction made rafts a less favorable environment for P-gp, which was sensitive to its lipid environment. We hypothesized that as RTX binding with CD20

translocated P-gp out of lipid rafts and inactivated P-gp. The mechanism of this interaction among CD20, RTX, lipid rafts, and P-gp remains to be investigated. The cell signaling pathways that involve CD20 are still being elucidated. Their complexity and far-reaching consequences throughout the cell suggest possible downstream interaction with molecules involved in the action of P-gp. This downstream interaction may indirectly cause P-gp to translocate out of rafts and become inactivated, though the intersection has not yet been identified.

Future Directions

Future research will be aimed at refining regimens for the clinical use of RTX in combination with chemotherapy. The next step is to confirm the chemosensitization of Namalwa/MDR1 tumor cells in SCID mice and determine the optimal dose regimens of chemotherapeutic agents and RTX to achieve chemosensitization *in vivo*. If successful in mice, this approach would then be further evaluated in clinical trials. The development and testing of other CD20⁺, P-gp⁺ lymphoma cell lines, as well as the use of other chemotherapeutic agents would also provide more insights into both the mechanisms underlying RTX-mediated chemosensitization and the use of RTX in patients. Finally, defining the optimal timing of treatment with RTX and chemotherapy may help prevent the development of MDR cells in early disease.

Conclusions

While clinical experience with RTX has shown that it improves the outcome of chemotherapy, the mechanism(s) underlying this synergy remain unknown. The

discovery of a specific inhibitor of the P-gp pump in MDR tumor cells represents an important advance in designing future strategies to prevent or reverse MDR. Insights into the mechanisms underlying the interaction between P-gp and CD20 as well as P-gp and CD19 [68] might facilitate the development of other targeted chemosensitizing agents, which would decrease the morbidity and mortality of patients with NHL. Optimization of therapeutic regimens that include RTX might also reduce the doses, and hence the side effects, of chemotherapeutic drugs necessary to achieve remission in patients. All these areas remain to be explored.

REFERENCES

1. Armitage, J.O. and D.L. Longo, *Harrison's online*, in *Malignancies of Lymphoid Cells Biology of Lymphoid Malignancies Concepts of the WHO Classification of Lymphoid Malignancies*, D.L. Kasper, et al., Editors. 2005, McGraw Hill.
2. Harris, N.L., et al., *World Health Organization classification of neoplastic diseases of the hematopoietic and lymphoid tissues: Report of the Clinical Advisory Committee Meeting, Airlie House, Virginia, November, 1997*. J Clin Oncol, 1999. **17**(12): p. 3835-49.
3. Armitage, J.O. and D.L. Longo, *Harrison's online*, in *Malignancies of Lymphoid Cells General Aspects of Lymphoid Malignancies*, D.L. Kasper, et al., Editors. 2005, McGraw Hill.
4. Von Mehren, M. and L.M. Weiner, *Monoclonal antibody therapy for cancer*. Annual Reviews in Medicine, 2003. **54**: p. 343-369.
5. Clynes, R.A., et al., *Inhibitory Fc receptors modulate in vivo cytotoxicity against tumor targets*. Nature Medicine, 2000. **6**(4): p. 443-446.
6. Von Mehren, M. and L.M. Weiner, *Monoclonal antibody-based therapy*. Current Opinion in Oncology, 1996. **8**: p. 493-498.
7. Carter, P., *Improving the efficacy of antibody-based cancer therapies*. Nature Reviews Cancer, 2001. **1**: p. 118-129.
8. Forero, A. and A.F. LoBuglio, *History of antibody therapy for non-Hodgkin's lymphoma*. Seminars in Oncology, 2003. **30**: p. 1-5.
9. Robak, T., *Monoclonal antibodies in the treatment of chronic lymphoid leukemias*. Leukemia & Lymphoma, 2004. **45**: p. 205-219.

10. Kaklamani, V. and R.M. O'Reagan, *New targeted therapies in breast cancer*. Seminars in Oncology, 2004. **31**: p. 20-25.
11. Veronese, M.L. and P.J. O'Dwyer, *Monoclonal antibodies in the treatment of colorectal cancer*. European Journal of Cancer, 2004. **40**: p. 1292-1301.
12. American Cancer Society. *Monoclonal Antibody Therapy (Passive Immunotherapy)*. 2004 2005/4/11 [cited 2005; Available from: http://www.cancer.org/docroot/ETO/content/ETO_1_4X_Monoclonal_Antibody_Therapy_Passive_Immunotherapy.asp?sitearea=ETO.
13. Hagenbeek, A. and V. Lewington, *Report of a European consensus workshop to develop recommendations for the optimal use of (90)Y-ibritumomab tiuxetan (Zevalin) in lymphoma*. Ann Oncol, 2005. **16**(5): p. 786-792.
14. Vose, J.M., *Bexxar: novel radioimmunotherapy for the treatment of low-grade and transformed low-grade non-Hodgkin's lymphoma*. Oncologist, 2004. **9**(2): p. 160-172.
15. Nuckel, H., et al., *Alemtuzumab induces enhanced apoptosis in vitro in B-cells from patients with chronic lymphocytic leukemia by antibody-dependent cellular cytotoxicity*. Eur J Pharmacol, 2005. **514**: p. 217-224.
16. Wang, Y., et al., *Biological activity of bevacizumab, a humanized anti-VEGF antibody in vitro*. Angiogenesis, 2004. **7**: p. 335-45.
17. Gennari, R., et al., *Pilot study of the mechanism of action of preoperative trastuzumab in patients with primary operable breast tumors overexpressing HER2*. Clin Cancer Res, 2004. **10**: p. 5650-5.

18. Midgley, R. and D. Kerr, *Bevacizumab--current status and future directions*. Ann Oncol, 2005. **16**: p. 999-1004.
19. Csapo, Z., et al., *Campath-1H as Rescue Therapy for the Treatment of Acute Rejection in Kidney Transplant Patients*. Transplant Proc, 2005. **37**: p. 2032-6.
20. Wiedmann, M.W. and K. Caca, *Molecularly targeted therapy for gastrointestinal cancer*. Curr Cancer Drug Targets, 2005. **5**: p. 171-93.
21. Goldstein, L.J., et al., *Expression of a multidrug resistance gene in human cancers*. Journal National Cancer Institute, 1989. **81**: p. 116-124.
22. Pileri, S.A., et al., *Immunohistochemical detection of the multidrug transport protein P170 in human normal tissues and malignant lymphomas*. Histopathology, 1991. **19**(2): p. 131-40.
23. Yang, X., et al., *Correlation of expression levels of multidrug resistance gene 1 (mdr1) mRNA, multidrug resistance-associated protein (MRP), and P-glycoprotein (P-gp) with chemotherapy efficacy in malignant lymphomas*. Zhonghua Yi Xue Za Zhi, 2002. **82**: p. 1177-9.
24. Ferte, J., *Analysis of the tangled relationships between P-glycoprotein-mediated multidrug resistance and the lipid phase of the cell membrane*. Eur J Biochem, 2000. **267**: p. 277-294.
25. Doige, C.A. and G.F. Ames, *ATP-dependent transport systems in bacteria and humans: relevance to cystic fibrosis and multidrug resistance*. Annu Rev Microbiol, 1993. **47**: p. 291-319.
26. Sikic, B.I., et al., *Modulation and prevention of multidrug resistance by inhibitors of P-glycoprotein*. Cancer Chemother Pharmacol, 1997. **40**(Suppl): p. S13-S19.

27. Vossebeld, P.J.M. and P. Sonneveld, *Reversal of multidrug resistance in hematological malignancies*. Blood Reviews, 1999. **13**: p. 67-78.
28. Ghetie, M.A., H. Bright, and E.S. Vitetta, *Homodimers but not monomers of Rituxan (chimeric anti-CD20) induce apoptosis in human B-lymphoma cells and synergize with a chemotherapeutic agent and an immunotoxin*. Blood 2001. **97**(5): p. 1392-8.
29. Grillo-Lopez, A.J., et al., *Overview of the clinical development of rituximab: first monoclonal antibody approved for the treatment of lymphoma*. Semin Oncol, 1999. **26**: p. 66-73.
30. Gopal, A.K. and O.W. Press, *Clinical applications of anti-CD20 antibodies*. J Lab Clin Med, 1999. **134**: p. 445-50.
31. McLaughlin, P., et al., *Rituximab chimeric anti-CD20 monoclonal antibody therapy for relapsed indolent lymphoma: half of patients respond to a four-dose treatment program*. J Clin Oncol, 1998. **16**: p. 2825-33.
32. Czuczman, M.S., et al., *Treatment of patients with low-grade B-cell lymphoma with the combination of chimeric anti-CD20 monoclonal antibody and CHOP chemotherapy*. J Clin Oncol, 1999. **17**: p. 268-76.
33. Czuczman, M.S., et al., *Prolonged clinical and molecular remission in patients with low-grade or follicular non-Hodgkin's lymphoma treated with rituximab plus CHOP chemotherapy: 9-year follow-up*. J Clin Oncol, 2004. **22**(23): p. 4711-6.
34. Feugier, P., et al., *Long-Term Results of the R-CHOP Study in the Treatment of Elderly Patients With Diffuse Large B-Cell Lymphoma: A Study by the Groupe d'Etude des Lymphomes de l'Adulte*. J Clin Oncol, 2005. **23**: p. 4117-26.

35. Zinzani, P.L., *Traditional treatment approaches in B-cell non-Hodgkin's lymphoma*. Leuk Lymphoma, 2003. **44**(Suppl 4): p. S6-S14.
36. Maloney, D.G., B. Smith, and F.R. Appelbaum, *The antitumor effect of monoclonal anti-CD20 antibody (mAb) therapy includes direct anti-proliferative activity and induction of apoptosis in CD20 positive non-Hodgkin's lymphoma (NHL) cell lines*. Blood, 1996. **88**(Suppl 1): p. 63.
37. Demidem, A., et al., *Chimeric anti-CD20 (IDEC-C2B8) monoclonal antibody sensitizes a B cell lymphoma cell line to cell killing by cytotoxic drugs*. Cancer Biother Radiopharm, 1997. **12**: p. 177-186.
38. Taji, H., et al., *Growth inhibition of CD20-positive B lymphoma cell lines by IDECC2B8 anti-CD20 monoclonal antibody*. Jpn J Cancer Res, 1998. **89**: p. 748-756.
39. Berchem, G.J., et al., *Rituximab induces caspase 3 mediated apoptosis of B-CLL cells despite rapid internalization of the CD20 protein* Proc Am Assoc Cancer Res, 2000. **41**: p. 826.
40. Niitsu, N., et al., *Phase I study of Rituximab-CHOP regimen in combination with granulocyte colony-stimulating factor in patients with follicular lymphoma*. Clinical Cancer Research, 2004. **10**: p. 4077-82.
41. Gluck, W.L., et al., *Phase I studies of Interleukin (IL)-2 and Rituximab in B-cell non-hodgkin's lymphoma: IL-2 mediated natural killer cell expansion correlations with clinical response*. Clinical Cancer Research, 2004. **10**: p. 2253-64.

42. Buske, C., et al., *Transplantation strategies for patients with follicular lymphoma*. Curr Opin Hematol, 2005. **12**: p. 266-72.
43. Chang, K.L., D.A. Arber, and L.M. Weiss, *CD20: A Review*. Applied Immunohistochemistry, 1996. **4**: p. 1-15.
44. Tedder, T.F. and P. Engel, *CD20: a regulator of cell-cycle progression of B lymphocytes*. Immunology Today, 1994. **15**: p. 450-454.
45. Bubien, J.K., et al., *Transfection of the CD20 cell surface molecule into ectopic cell types generates a Ca²⁺ conductance found constitutively in B lymphocytes*. J Cell Biol, 1993. **121**: p. 1121-1132.
46. Polyak, M.J. and J.P. Deans, *Alanine-170 and proline-172 are critical determinants for extracellular CD20 epitopes; heterogeneity in the fine specificity of CD20 monoclonal antibodies is defined by additional requirements imposed by both amino acid sequence and quaternary structure*. Blood, 2002. **99**: p. 3256-3262.
47. Li, H., et al., *Store-operated Cation Entry Mediated by CD20 in Membrane Rafts*. Journal of Biological Chemistry, 2003. **278**: p. 42427-42434.
48. Cragg, M.S. and M.J. Glennie, *Antibody specificity controls in vivo effector mechanisms of anti-CD20 reagents*. Blood, 2004. **103**: p. 2738-2743.
49. Rajendran, L. and K. Simons, *Lipid rafts and membrane dynamics*. J Cell Sci, 2005. **118**: p. 1099-1102.
50. Schuck, S., et al., *Resistance of cell membranes to different detergents*. Proc Natl Acad Sci, 2003. **100**: p. 5795-5800.

51. Simons, K. and W.L. Vaz, *Model systems, lipid rafts, and cell membranes*. Annu Rev Biophys Biomol Struct, 2004. **33**: p. 269-295.
52. Chatterjee, S. and S. Mayor, *The GPI anchor and protein sorting*. Cell Mol Life Sci, 2001. **58**: p. 1969-1987.
53. Simons, K. and D. Toomre, *Lipid rafts and signal transduction*. Nat Rev Mol Cell Biol, 2000. **1**: p. 31-39.
54. Rajendran, L., et al., *Asymmetric localization of flotillins/reggies in preassembled platforms confers inherent polarity to hematopoietic cells*. Proc Natl Acad Sci, 2003. **100**: p. 8241-6.
55. Kurzchalia, T.V. and R.G. Parton, *Membrane microdomains and caveolae*. Curr Opin Cell Biol, 1999. **11**: p. 424-431.
56. Babiychuk, E.B., et al., *Modulating signaling events in smooth muscle: cleavage of annexin 2 abolishes its binding to lipid rafts*. FASEB J, 2002. **16**: p. 1177-1184.
57. Deans, J.P., et al., *Rapid redistribution of CD20 to a low-density detergent-insoluble membrane compartment*. J Biol Chem, 1998. **273**: p. 344-8.
58. Petrie, R.J. and J.P. Deans, *Colocalization of the B cell receptor and CD20 followed by activation-dependent dissociation in distinct lipid rafts*. Journal of Immunology, 2002. **169**(6): p. 2886-91.
59. Semac, I., et al., *Anti-CD20 therapeutic antibody rituximab modifies the functional organization of rafts/microdomains of B lymphoma cells*. Cancer Research, 2003. **63**(2): p. 534-40.

60. Li, H., et al., *The CD20 calcium channel is localized to microvilli and constitutively associated with membrane rafts: antibody binding increases the affinity of the association through an epitope-dependent cross-linking-independent mechanism.* J Biol Chem, 2004. **279**(19): p. 19893-901.
61. Luker, G.D., et al., *Effects of cholesterol and enantiomeric cholesterol on P-glycoprotein localization and function in low-density membrane domains.* Biochemistry, 2000. **39**(26): p. 7651-61.
62. Bacso, Z., et al., *Raft and cytoskeleton associations of an ABC transporter: P-glycoprotein.* Cytometry Part A: The Journal of the International Society for Analytical Cytology, 2004. **61**(2): p. 105-16.
63. Garrigues, A., A.E. Escargueil, and S. Orlowski, *The multidrug transporter, P-glycoprotein, actively mediates cholesterol redistribution in the cell membrane.* Proceedings of the National Academy of Sciences, 2002. **99**(16): p. 10347-52.
64. Modok, S., C. Heyward, and R. Callaghan, *P-glycoprotein retains function when reconstituted into a sphingolipid- and cholesterol-rich environment.* Journal of Lipid Research, 2004. **45**(10): p. 1910-8.
65. Troost, J., et al., *Modulation of cellular cholesterol alters P-glycoprotein activity in multidrug-resistant cells.* Molecular Pharmacology, 2004. **66**(5): p. 1332-9.
66. Gayet, L., et al., *Control of P-glycoprotein activity by membrane cholesterol amounts and their relation to multidrug resistance in human CEM leukemia cells.* Biochemistry, 2005. **44**(11): p. 4499-509.

67. Ghetie, M.-A., V. Ghetie, and E.S. Vitetta, *Anti-CD19 Antibodies Inhibit the Function of the P-gp Pump in Multidrug-resistant B Lymphoma Cells*. Clinical Cancer Research, 1999. **5**: p. 3920-27.
68. Ghetie, M.-A., et al., *An anti-CD19 antibody inhibits the interaction between P-glycoprotein (P-gp) and CD19, causes P-gp to translocate out of lipid rafts, and chemosensitizes a multidrug-resistant (MDR) lymphoma cell line*. Blood, 2004. **104**: p. 178-83.
69. Klein, G., et al., *An EBV-genome-negative cell line established from an American Burkitt lymphoma; receptor characteristics. EBV infectibility and permanent conversion into EBV-positive sublines by in vitro infection*. Intervirology, 1975. **5**: p. 319-334.
70. Tsuruo, T., et al., *Overcoming of Vincristine resistance in P388 leukemia in vivo and in vitro through enhanced cytotoxicity of Vincristine and vinblastine by Verapamil*. Cancer Research, 1981. **41**: p. 1967-1972.
71. MacDonald, J. and L. Pike, *A simplified method for the preparation of detergent-free lipid rafts*. Journal of Lipid Research, 2005. **46**: p. 1061-1067.
72. Gaus, K., et al., *Domain-specific lipid distribution in macrophage plasma membranes*. Journal of Lipid Research, 2005. **46**: p. 1526-1538.
73. Smart, E., et al., *A detergent-free method for purifying caveolae membrane from tissue culture cells*. Proceedings of the National Academy of Science, USA, 1995. **92**: p. 10104-10108.
74. Maloney, D.G., B. Smith, and A. Rose, *Rituximab: Mechanism of Action and Resistance*. Seminars in Oncology, 2002. **29**(Suppl 2): p. 2-9.

75. Bezombes, C., et al., *Rituximab antiproliferative effect in B-lymphoma cells is associated with acid-sphingomyelinase activation in raft microdomains*. Blood, 2004. **104**: p. 1166-73.
76. Rose, A.L., B.E. Smith, and D.G. Maloney, *Glucocorticoids and rituximab in vitro: synergistic direct antiproliferative and apoptotic effects*. Blood, 2002. **100**: p. 1765-73.
77. Liu, C., et al., *Antilymphoma Effects of Anti-HLA-DR and CD20 Monoclonal Antibodies (Lym-1 and Rituximab) on Human Lymphoma Cells*. Cancer Biotherapy and Radiopharmaceuticals, 2004. **19**: p. 545-61.
78. Shan, D., J.A. Ledbetter, and O.W. Press, *Apoptosis of Malignant Human B Cells by Ligation of CD20 With Monoclonal Antibodies*. Blood, 1998. **91**: p. 1644-52.
79. Bonavida, B. and M.I. Vega, *Rituximab-mediated chemosensitization of AIDS and non-AIDS non-Hodgkin's Lymphoma*. Drug Resistance Updates, 2005. **8**: p. 27-41.
80. Deans, J.P., et al., *Association of 75/80-kDa phosphoproteins and the tyrosine kinases Lyn, Fyn, and Lck with the B cell molecule CD20. Evidence against involvement of the cytoplasmic regions of CD20*. J Biol Chem, 1995. **270**: p. 22632-22638.
81. Deans, J.P., H. Li, and M.J. Polyak, *CD20-mediated apoptosis: signaling through lipid rafts*. Immunology, 2002. **107**: p. 176-82.
82. Ghetie, M.-A., et al., *Rituximab but not other anti-CD20 antibodies reverses multidrug resistance in two B lymphoma cell lines, blocks the activity of P-*

- glycoprotein (P-gp), and induces P-gp to translocate out of lipid rafts. Clinical Cancer Research, Submitted November 2005.*
83. Murren, J.R., *Modulating Multidrug Resistance: Can We Target this Therapy?* Clinical Cancer Research, 2002. **8**: p. 633-5.
 84. Cragg, M.S., et al., *Complement-mediated lysis by anti-CD20 MAb correlates with segregation into lipid rafts.* Blood, 2003. **101**: p. 1045-52.
 85. Unruh, T.L., et al., *Cholesterol depletion inhibits src family kinase-dependent calcium mobilization and apoptosis induced by rituximab crosslinking.* Immunology, 2005. **116**(2): p. 223-32.
 86. Janas, E., et al., *Rituxan (anti-CD20 antibody)-induced translocation of CD20 into lipid rafts is crucial for calcium influx and apoptosis.* Clinical and Experimental Immunology, 2005. **139**: p. 439-446.
 87. Polyak, M.J., et al., *A cholesterol-dependent CD20 epitope detected by the FMC7 antibody.* Leukemia, 2003. **17**: p. 1384-9.
 88. Holder, M.J., et al., *Improved access to CD20 following B cell receptor cross-linking at Burkitt's lymphoma cell surfaces.* Leukemia Research, 2004. **28**: p. 1197-1202.

VITAE

Michelle C. Crank was born in San Antonio, Texas on January 24, 1979 to Charles and Susan Crank. After graduating as valedictorian from St. Mary's Hall high school in San Antonio in 1997, she entered Princeton University in Princeton, New Jersey. During the summers of 1999 and 2000, she worked as a research assistant with Dr. Peter Fox, M.D., at the Research Imaging Center (RIC) at the University of Texas (UT) Health Science Center, San Antonio. Her work studying the imaging literature on Broca's Area resulted in co-authorship of an article for Academic Press' *Encyclopedia of the Human Brain* entitled "Broca's Area."

During her junior and senior years at Princeton, she worked with Dr. Suzanne Walker in the Chemistry Department performing research for her senior thesis, entitled "The Binding of the Lantibiotic Nisin to Synthetic Substrate Analogues of Lipid II." She graduated Cum Laude with a Bachelor of Arts from Princeton University with a major in chemistry in June 2001.

During the following year, she returned to the RIC, where she helped design and create an online database for neuroimaging literature. She traveled to neuroimaging departments across the country to promote and demonstrate the database, and she co-authored the users manual.

In June 2002, Michelle began the first of two summers participating in the Medical Student Summer Research Program at the Cancer Immunobiology Center at UT Southwestern Medical Center. In September 2002, she began medical school at UT Southwestern. Since that time, she has presented research posters at the Medical Student Research Forum at UT Southwestern in 2003 and 2004, and in 2004 was chosen to give

an oral presentation. She co-chaired the 2005 Medical Student Research Forum. In addition, Michelle was a student liaison for the medical school immunology course.

After graduation from medical school, Michelle plans to pursue residency training in Internal Medicine and a career in academic medicine.

Permanent Address:

2915 Oak Falls

San Antonio, TX 78231

PUBLICATIONS

1. Crank, M. C. The Binding of the Lantibiotic Nisin to Synthetic Substrate Analogues of Lipid II. Senior Thesis in the Department of Chemistry, Princeton University, May 2001.
2. Crank, M., and Fox, P. T. "Broca's Area." In: *Encyclopedia of the Human Brain*. Vol. 1. Ed: V. S. Ramachandran, Academic Press, San Diego, CA, pp. 569-586, 2002.
3. Fox, P. T., Laird, A. R., Fox, S. P., Fox, P. M., Uecker, A. M., Crank, M., Koenig, S. F., Lancaster, J. L. "BrainMap taxonomy of experimental design: description and evaluation," *Human Brain Mapping*, May 2005, Vol. 25, pp 185-98.
4. Ghetie, M-A., Crank, M., Kufert, S., Pop, I., and Vitetta, E. S. "Rituximab™ but not other anti-CD20 antibodies reverses multidrug resistance in two B lymphoma cell lines, blocks the activity of P-glycoprotein (P-gp), and induces P-gp to translocate out of lipid rafts." *Journal of Immunotherapy*. In press.